

The Pulsar Sequence

The Fundamental Plane of Gamma-Ray Pulsars: From Observations to PIC Models



Constantinos Kalapotharakos

NASA, Goddard Space Flight Center

University of Maryland College Park, CRESST II

Collaborators:

Alice Harding (NASA/GSFC)

Demos Kazanas (NASA/GSFC)

Zorawar Wadiasingh (NASA/GSFC, USRA)

Gabriele Brambilla (University of Milan, NASA/GSFC)

Andrey Timokhin (UMCP, NASA/GSFC)

**High Energy Phenomena in Relativistic Outflows VII
(HEPRO VII)**

HEPRO VII

HIGH ENERGY PHENOMENA IN RELATIVISTIC OUTFLOWS VII

BARCELONA, 9-12 JULY 2019

FACULTY OF PHYSICS

UNIVERSITY OF BARCELONA

<https://indico.icc.ub.edu/event/9/>

Contact: hepro7@icc.ub.edu

SCIENTIFIC ORGANIZING COMMITTEE

Felix Aharonian (DIAS/MPK)
Gennady Bisnovaty-Kogan (IKI)
Ioannis Contopoulos (Academy of Athens)
Alice Harding (NASA)
Dmitry Khangulyan (Rikkyo University)
Josep M. Paredes (Universitat de Barcelona/ICCUB, Chair)
Manel Perucho (Universitat de València)
Elena Pian (INAF)
Tsvi Piran (HUJI)
Nanda Rea (CSIC-IEEC)
Elisa Resconi (TUM)
Gustavo E. Romero (IAR/UNLP)
Samar Safi-Harb (University of Manitoba)
Megan C. Urry (Yale University)
Xiang-Yu Wang (Nanjing University)

LOCAL ORGANIZING COMMITTEE

Pol Bordas
Valentí Bosch-Ramon
Matteo Cerruti
Kazushi Iwasawa
Edgar Molina
Josep M. Paredes
Marc Ribó
Núria Torres-Albà



Outline

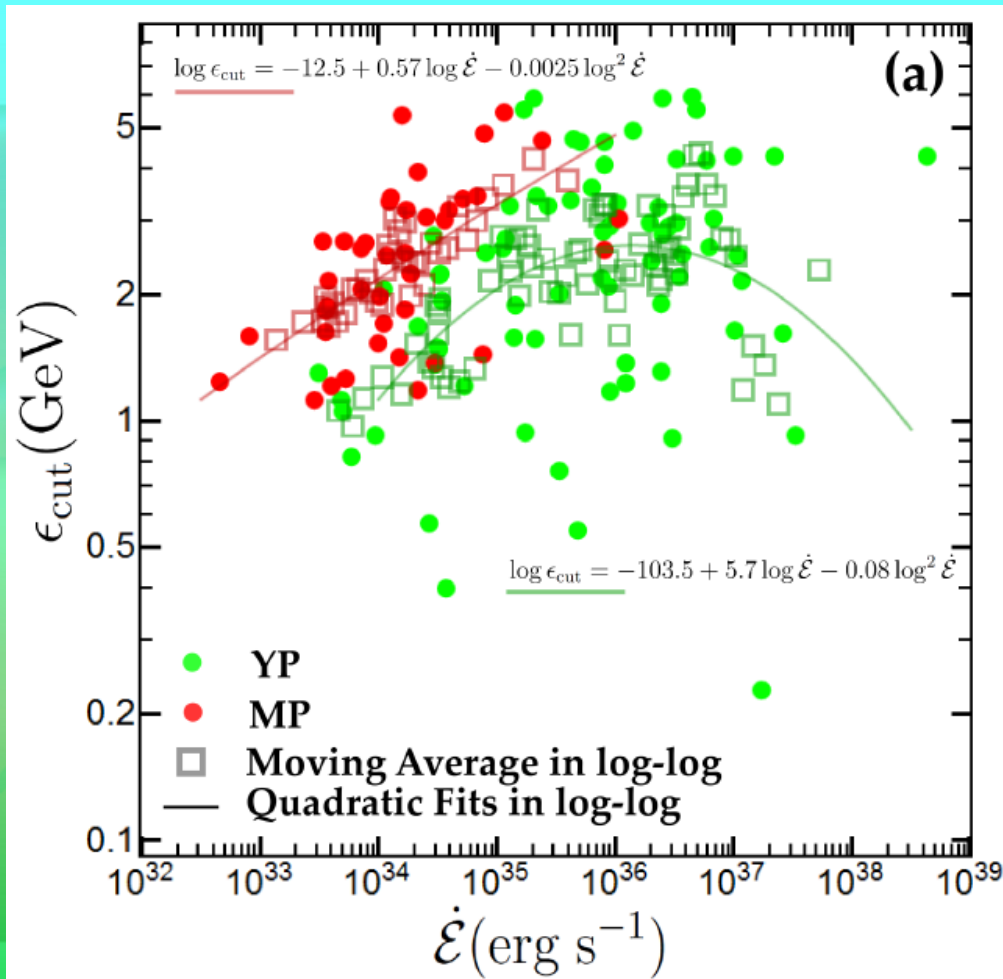
- Observations (FERMI)
- Orbital exploration CR vs SR
- Fundamental Plane of γ -ray Pulsars
- What PIC Global Models Say
- Summary

*Assumptions:
Eq. Cur. Sheet, LC
RRLR*

FERMI

$N_p \rightarrow \times 30$

$N_p > 230$ (117 in 2PC; Abdo et al. 2013)



Kalapotharakos et al. (2017)

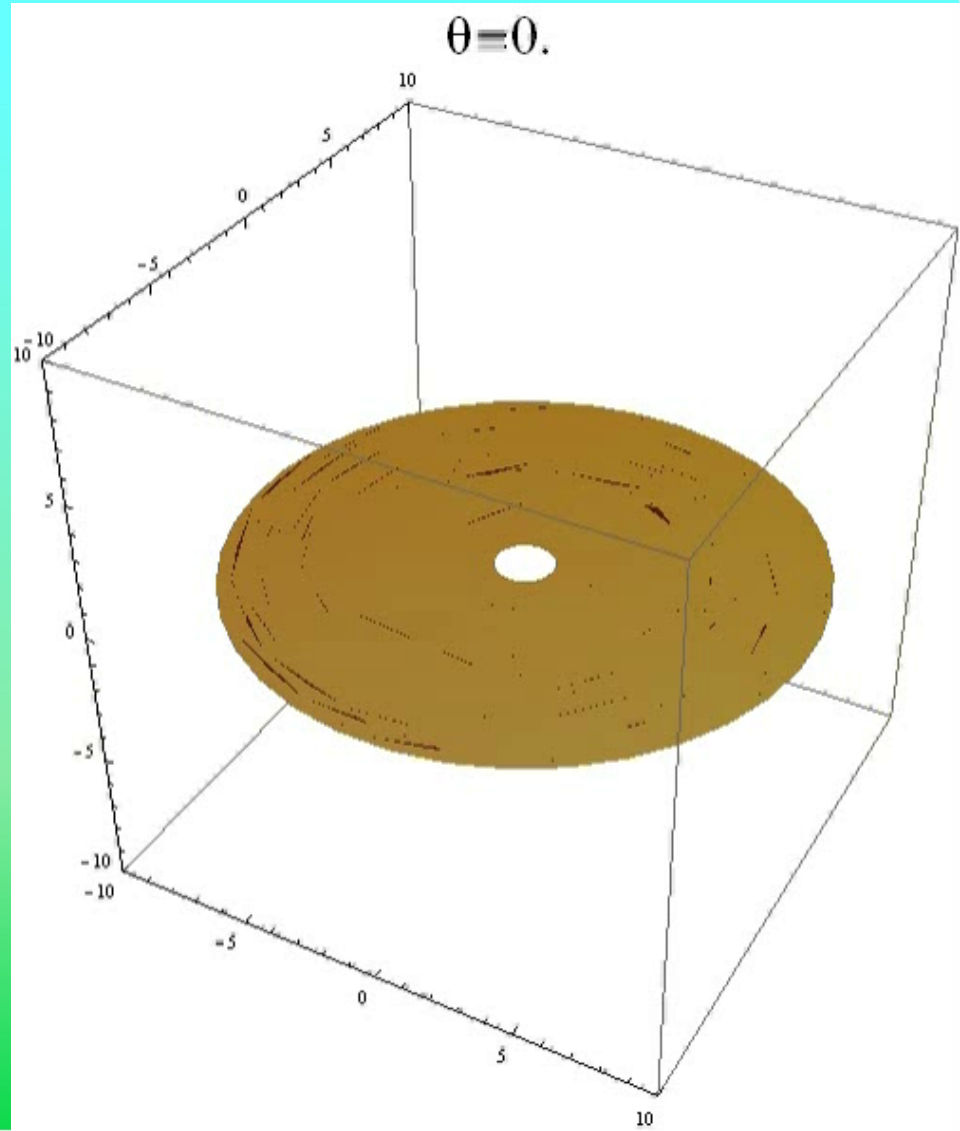
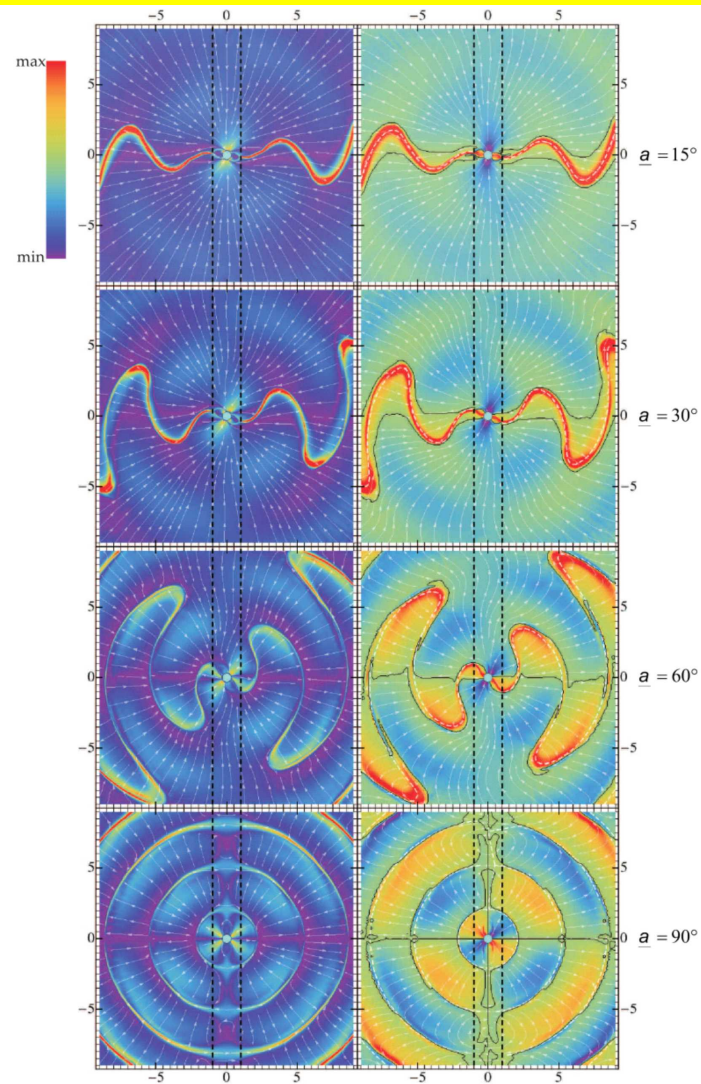
FFE Models

Contopoulos, Kazanas, & Fendt (1999)

Spitkovsky (2006)

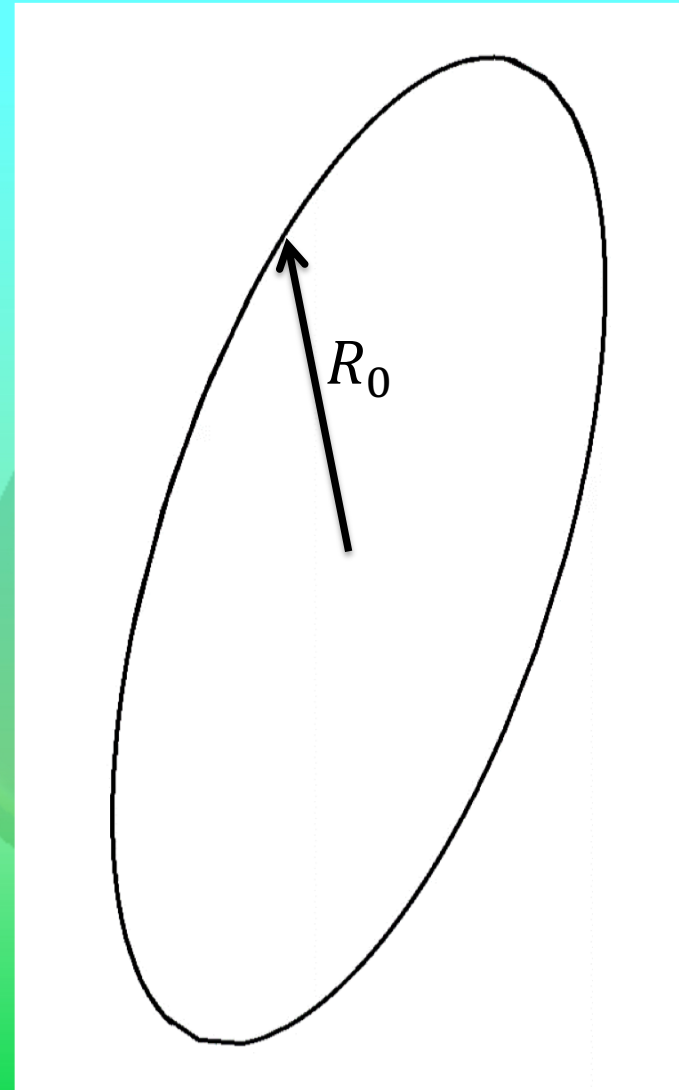
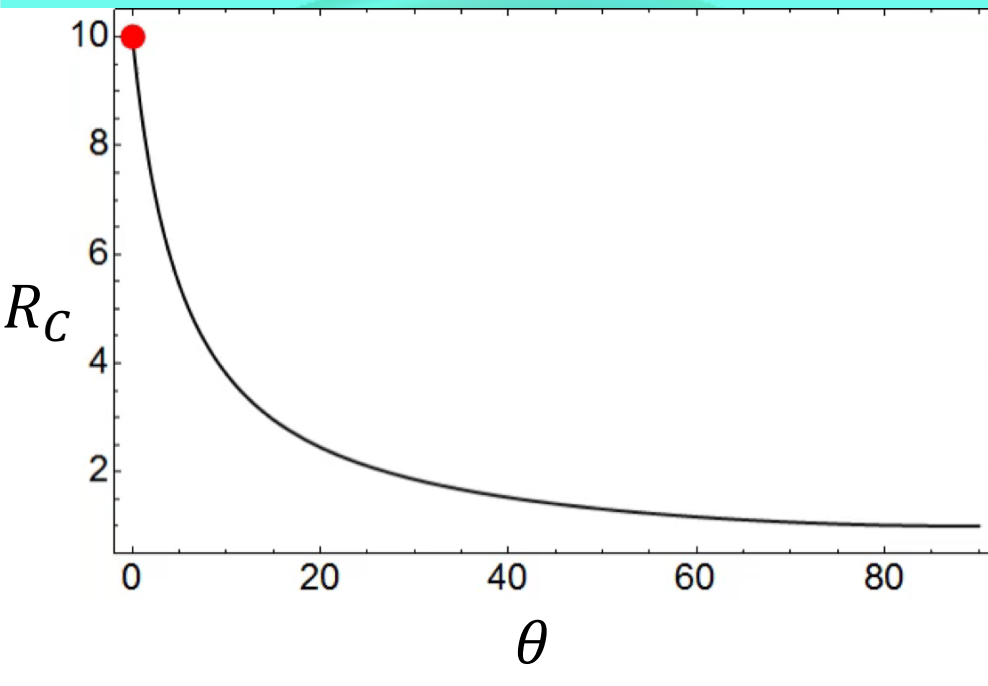
Kalapothisarakos et al. (2012)

Bogovalov (1999)



Orbital Exploration (SR \leftrightarrow CR)

$\theta = 0.0, R_c = 10.00$



Fundamental Plane (Theory)

Assumptions

1) Radiation Reaction Limit Regime

2) At the ECS near the LC

CR

Kalapothisarakos et al. (2019)

$$R_C \propto R_{LC} \propto P$$

$$B_{LC} \propto B_* R_{LC}^{-3} \propto B_* P^{-3}$$

$$\gamma_L \propto \epsilon^{1/3} P^{1/3}$$

$$E_{BLC} B_{LC} \propto \gamma_L^4 R_C^{-2}$$

$$E_{BLC} \propto \epsilon^{4/3} P^{7/3} B_*^{-1}$$

$$L_{\gamma 1} \propto \epsilon^{4/3} P^{-2/3}$$

$$\rho_{GJ} \propto B_* P^{-1}$$

$$\dot{\epsilon} \propto B_*^2 P^{-4}$$

$$L_\gamma \propto \epsilon_{cut}^{4/3} B_*^{1/6} \dot{\epsilon}^{5/12}$$

$$\frac{2q_e^2 \gamma_L^4}{3m_e c R_C^2(\theta)} = \frac{q_e \mathbf{v} \cdot \mathbf{E}}{m_e c^2}$$

$$\epsilon_{cut} = \frac{3}{2} c \hbar \frac{\gamma_L^3}{R_C(\theta)}$$

Fundamental Plane (Theory)

Assumptions

1) Radiation Reaction Limit Regime

2) At the ECS near the LC

Kalapothisarakos et al. (2019)

$$R_C \propto R_{LC} \propto P$$

$$B_{LC} \propto B_* R_{LC}^{-3} \propto B_* P^{-3}$$

$$\gamma_L \propto \epsilon_{cut}^{1/3} P^{1/3}$$

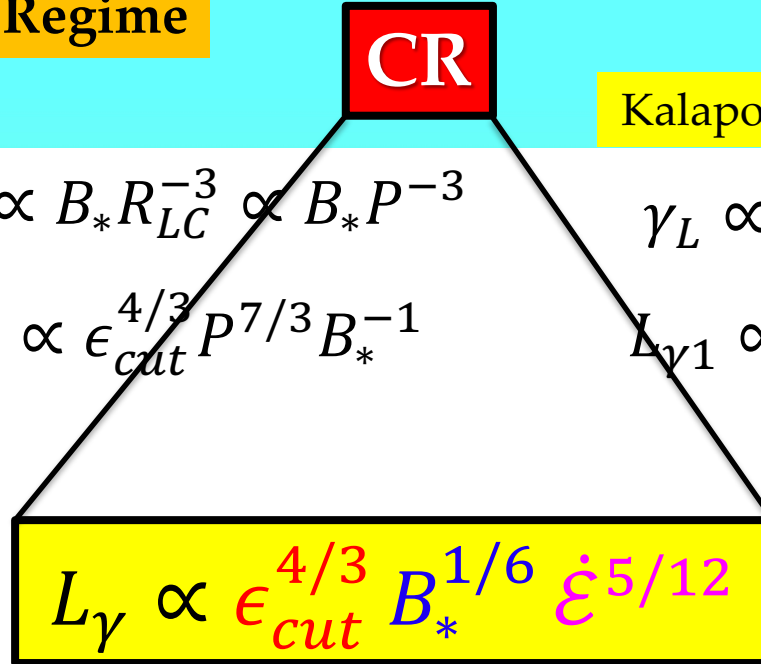
$$E_{BLC} B_{LC} \propto \gamma_L^4 R_C^{-2}$$

$$E_{BLC} \propto \epsilon_{cut}^{4/3} P^{7/3} B_*^{-1}$$

$$L_{\gamma 1} \propto \epsilon_{cut}^{4/3} P^{-2/3}$$

$$\rho_{GJ} \propto B_* P^{-1}$$

$$\dot{\xi} \propto B_*^2 P^{-4}$$



$$R_C \propto r_g \propto \gamma_L B_*^{-1} P^3$$

$$L_\gamma \propto \epsilon_{cut} \dot{\xi}$$

SR

Fundamental Plane (Observations)

88 Fermi YPs+MPs

$$L_{\gamma(3D)} = 10^{14.2 \pm 2.3} \epsilon_{cut}^{1.18 \pm 0.24} B_*^{0.17 \pm 0.05} \dot{\xi}^{0.41 \pm 0.08}$$

ϵ_{cut} (MeV), B_* (G), L_{γ} , $\dot{\xi}$ (erg/s)

Fermi data

Kalapotharakos et al. (2019)

$$L_{\gamma} \propto \epsilon_{cut}^{4/3} B_*^{1/6} \dot{\xi}^{5/12}$$

Theory CR

Fundamental Plane (Observations)

88 Fermi YPs+MPs

$$L_{\gamma(3D)} = 10^{14.2 \pm 2.3} \epsilon_{cut}^{1.18 \pm 0.24} B_*^{0.17 \pm 0.05} \dot{\xi}^{0.41 \pm 0.08}$$

ϵ_{cut} (MeV), B_* (G), L_{γ} , $\dot{\xi}$ (erg/s)

Fermi data

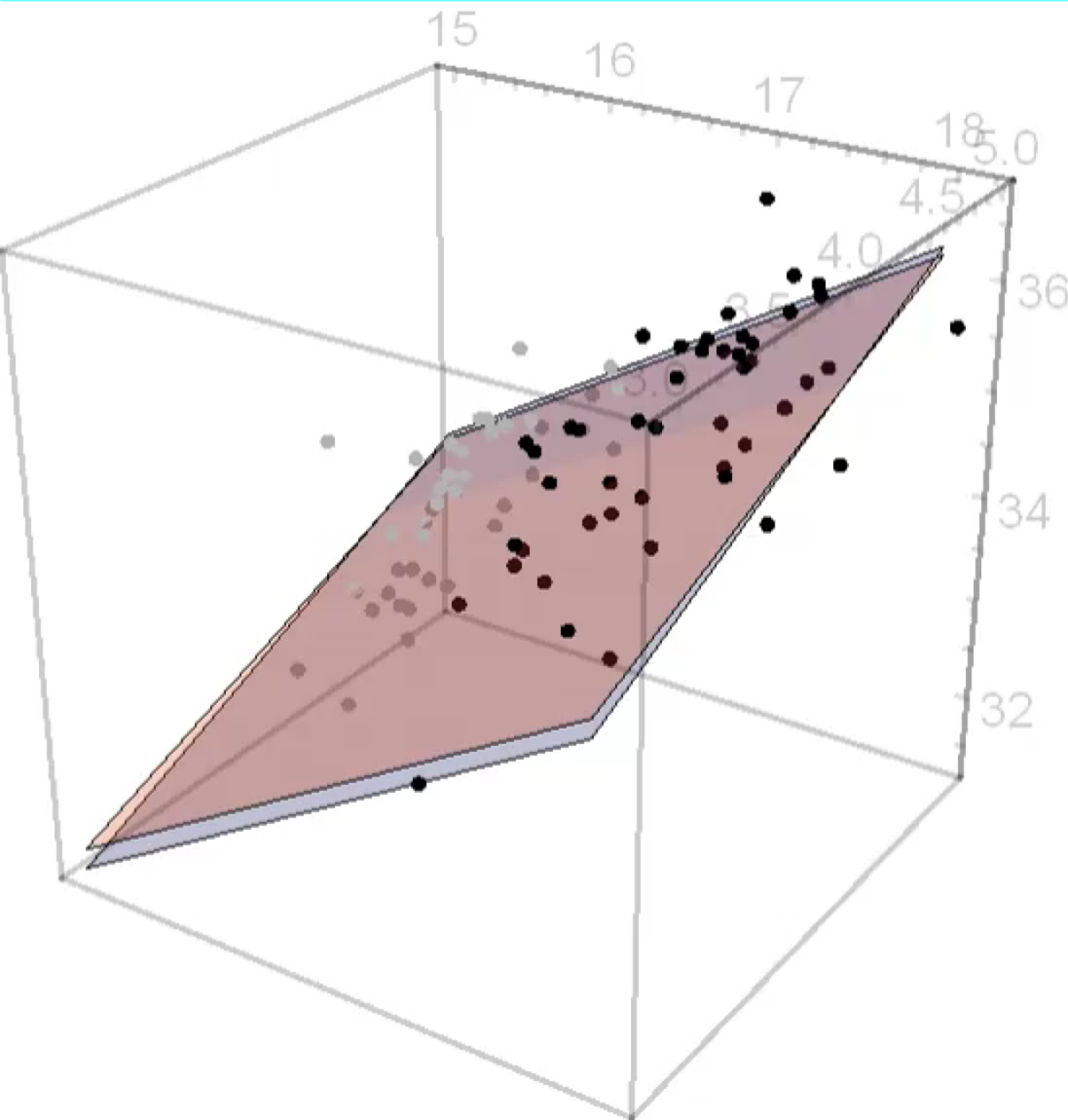
Kalapotharakos et al. (2019)

$$L_{\gamma} \propto \epsilon_{cut}^{4/3} B_*^{1/6} \dot{\xi}^{5/12}$$

Theory CR

Fundamental Plane (Observations)

4D-space is hard to visualize



$$\begin{aligned}x &= B_*^{1/6} \dot{\xi}^{5/12} \\y &= \epsilon_{cut}^{4/3} \\z &= L_\gamma\end{aligned}$$

$$z \propto x y$$

(Theory)

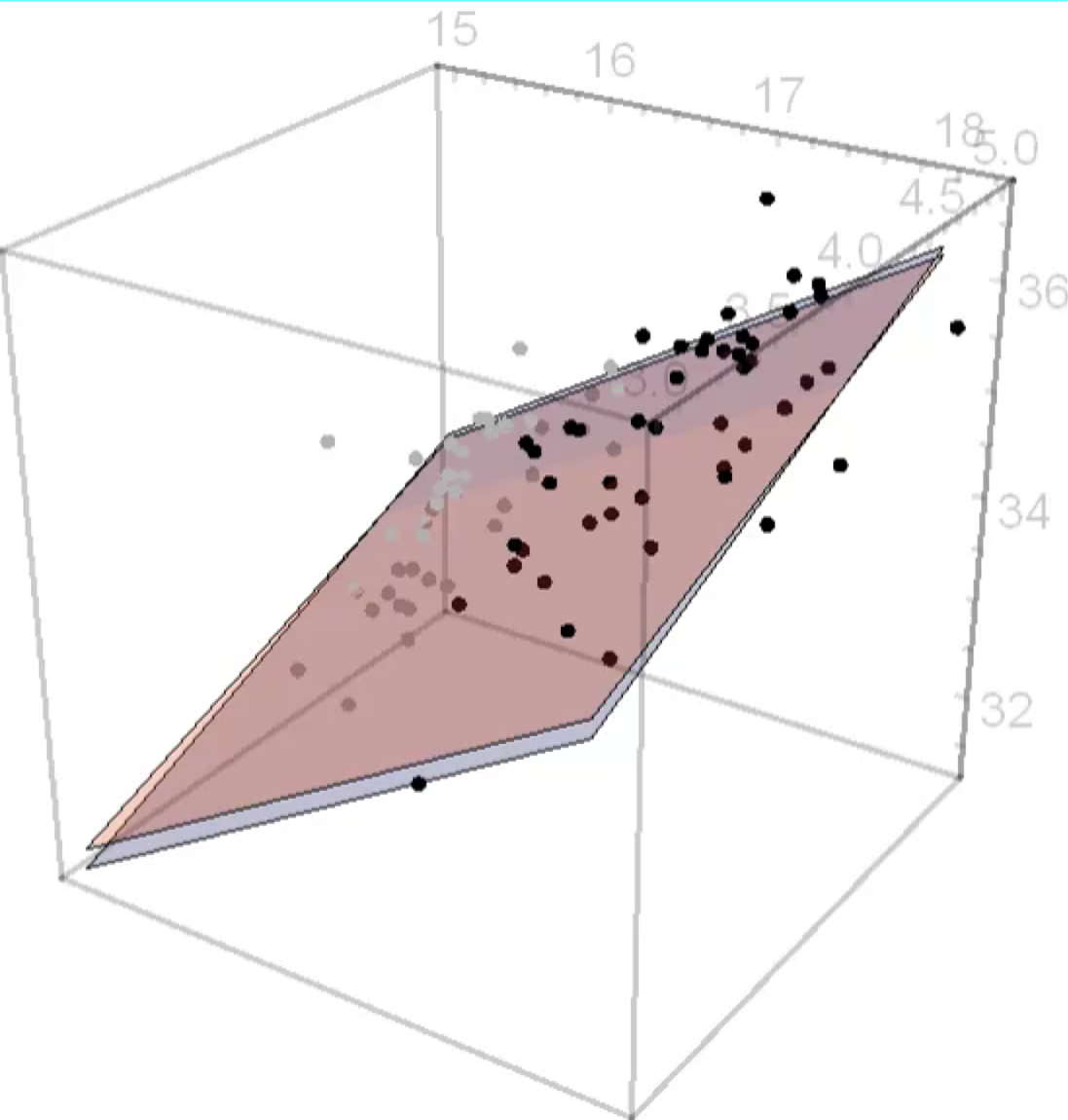
$$z \propto x^{0.99} y^{0.88}$$

(Fermi data)

- Fermi YP
- Fermi MP

Fundamental Plane (Observations)

4D-space is hard to visualize



$$\begin{aligned}x &= B_*^{1/6} \dot{\xi}^{5/12} \\y &= \epsilon_{cut}^{4/3} \\z &= L_\gamma\end{aligned}$$

$$z \propto x y$$

(Theory)

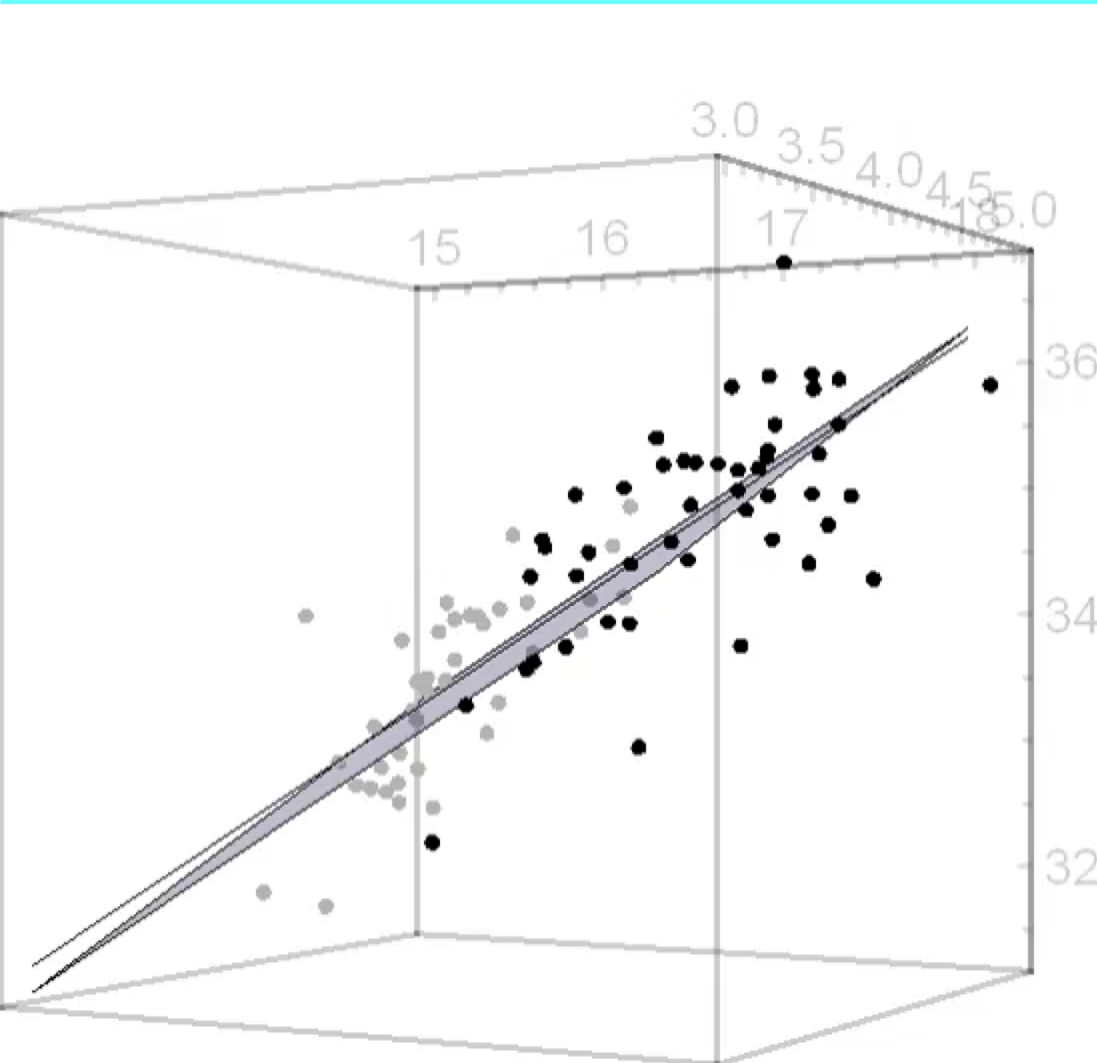
$$z \propto x^{0.99} y^{0.88}$$

(Fermi data)

- Fermi YP
- Fermi MP

Fundamental Plane (Observations)

4D-space is hard to visualize



$$x = B_*^{1/6} \dot{\xi}^{5/12}$$
$$y = \epsilon_{cut}^{4/3}$$
$$z = L_\gamma$$

$$z \propto x y$$

(Theory)

$$z \propto x^{0.99} y^{0.88}$$

(Fermi data)

- Fermi YP
- Fermi MP

3D Kinetic Models (PIC)

Kinetic PIC simulations provide a path to self-consistency.

Field structure & particle distributions are consistent to each other

3D Particle-In-Cell code

Kalapothisarakos et al. (2018)

Brambilla et al. (2018)

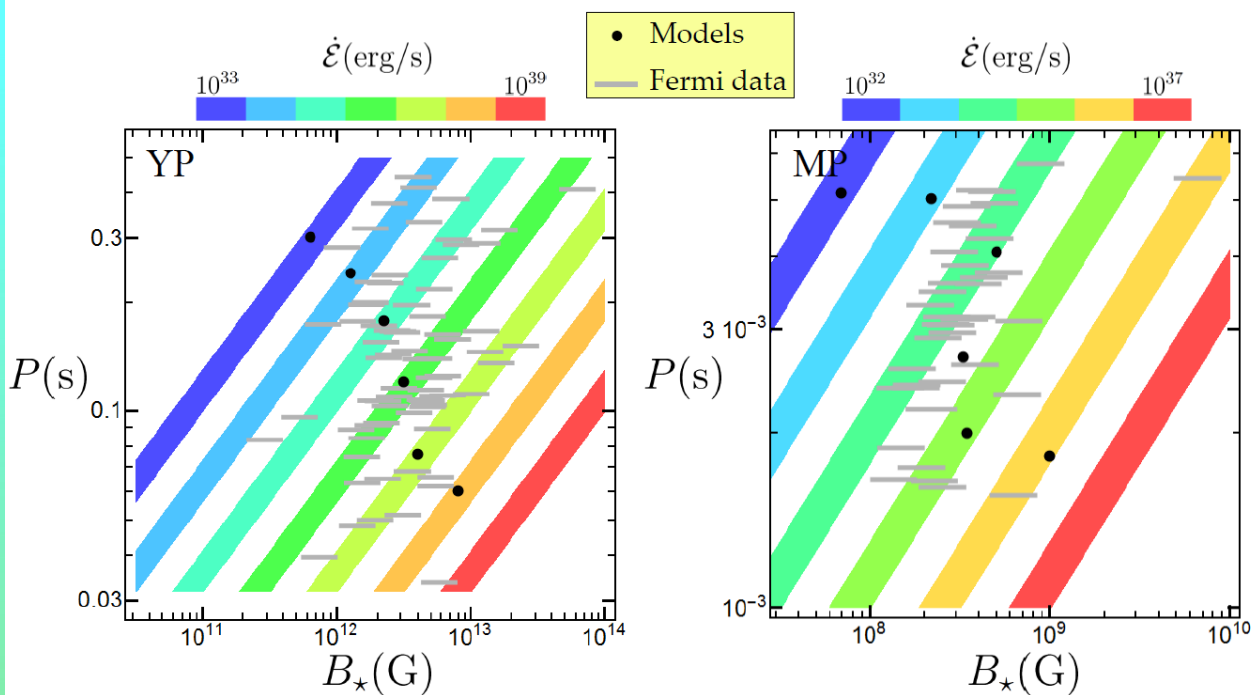
Kalapothisarakos et al. (2019, in prep)

C-3PA

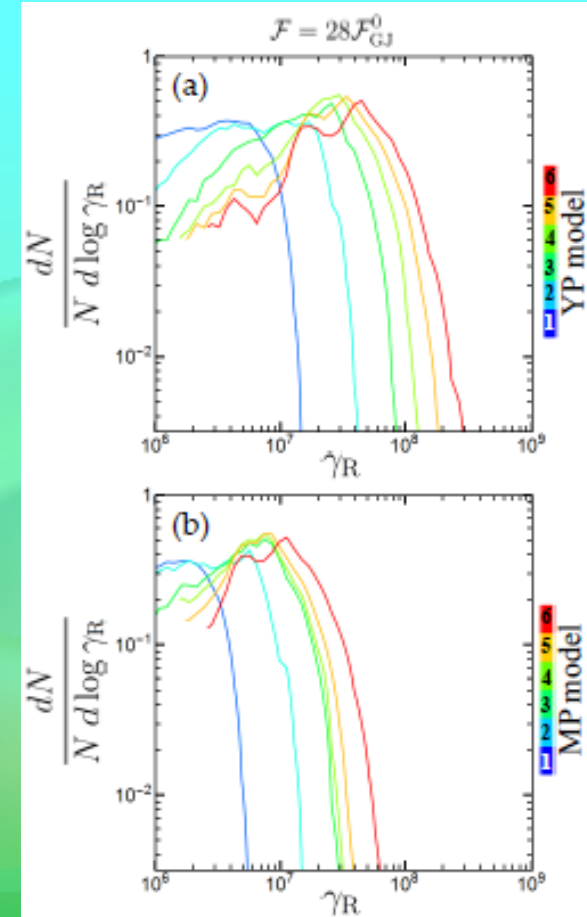
**Pleiades & Discover
Supercomputers, NASA**
~ 4000cpus
~ $10^7 - 10^9$ particles

- Cartesian
- Conservative
- Vay's algorithm
- Current Smoothing
- Radiation Reaction Forces
- Load Balancing
- Field Line Dependent Particle Injection

3D Kinetic Models (PIC)

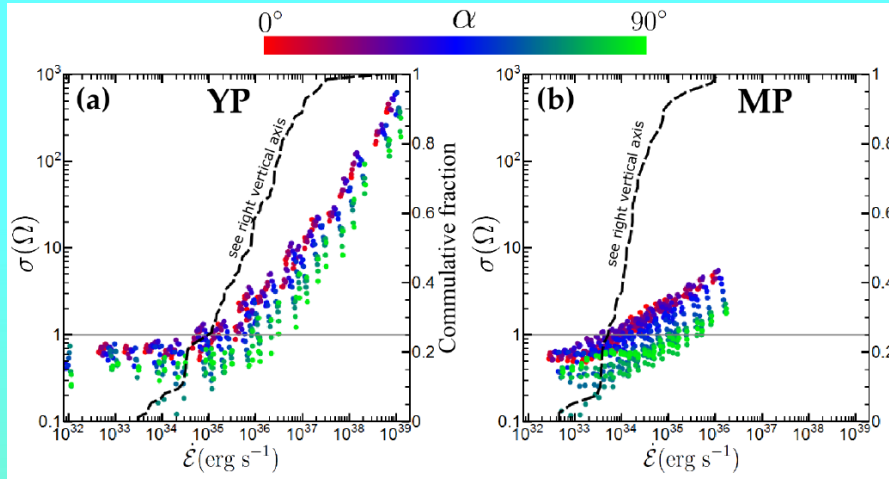


Kalapotharakos et al. (2018)



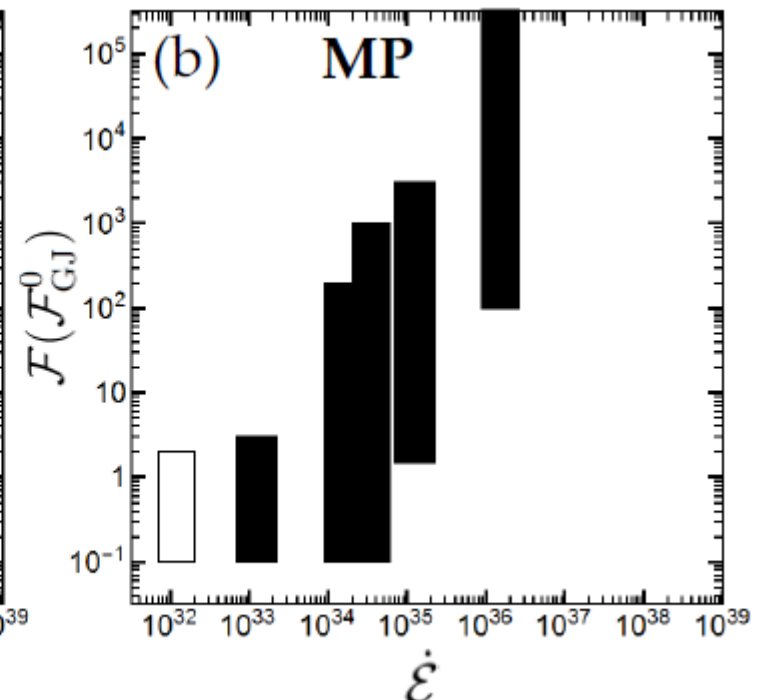
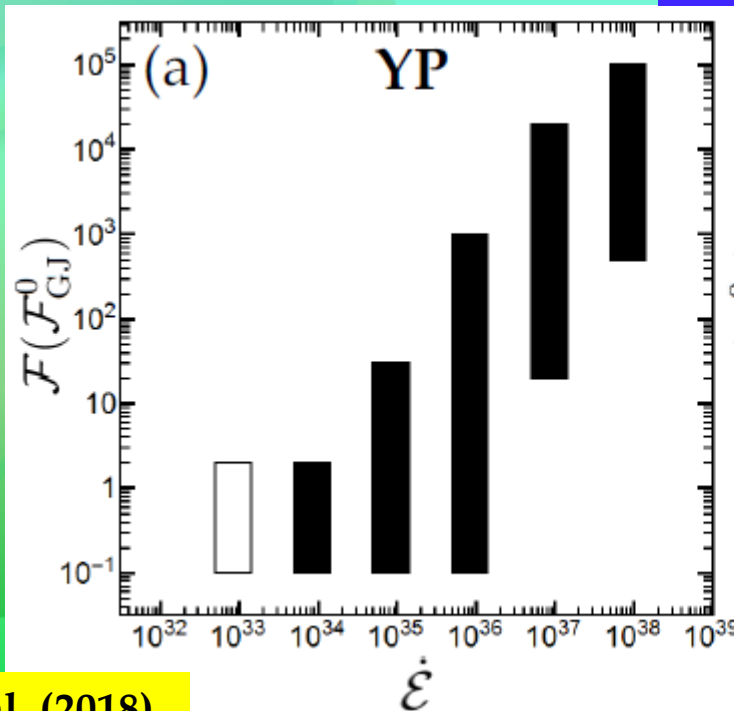
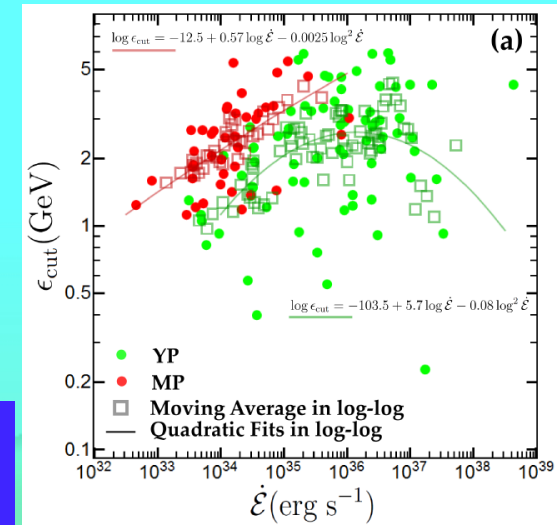
We scale-up the particle energies assuming realistic B and P values.

3D Kinetic Models (PIC)



$$\sigma(\dot{\mathcal{E}})$$

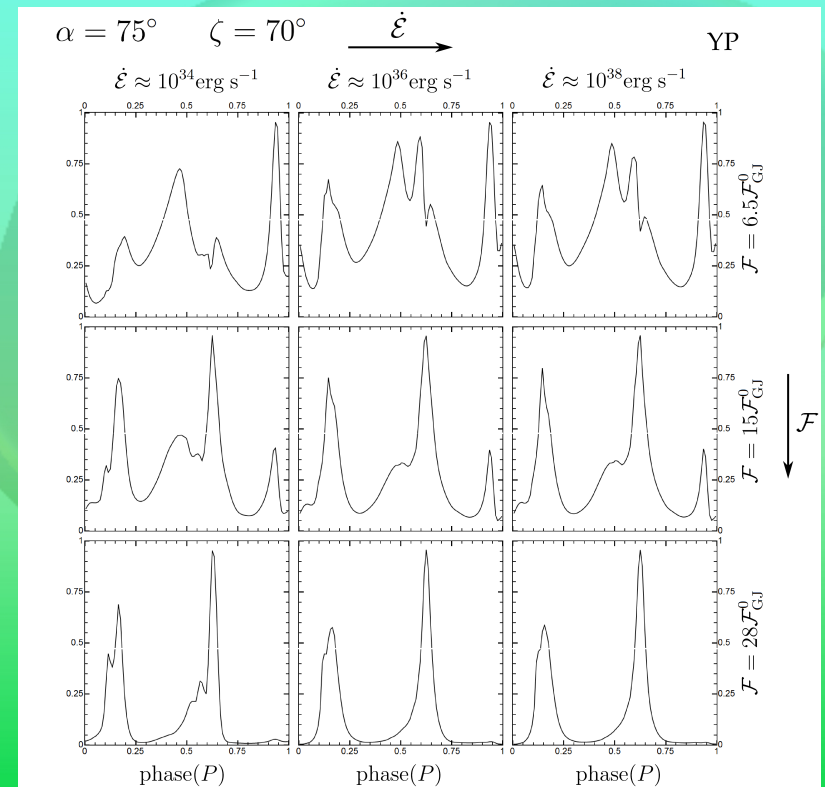
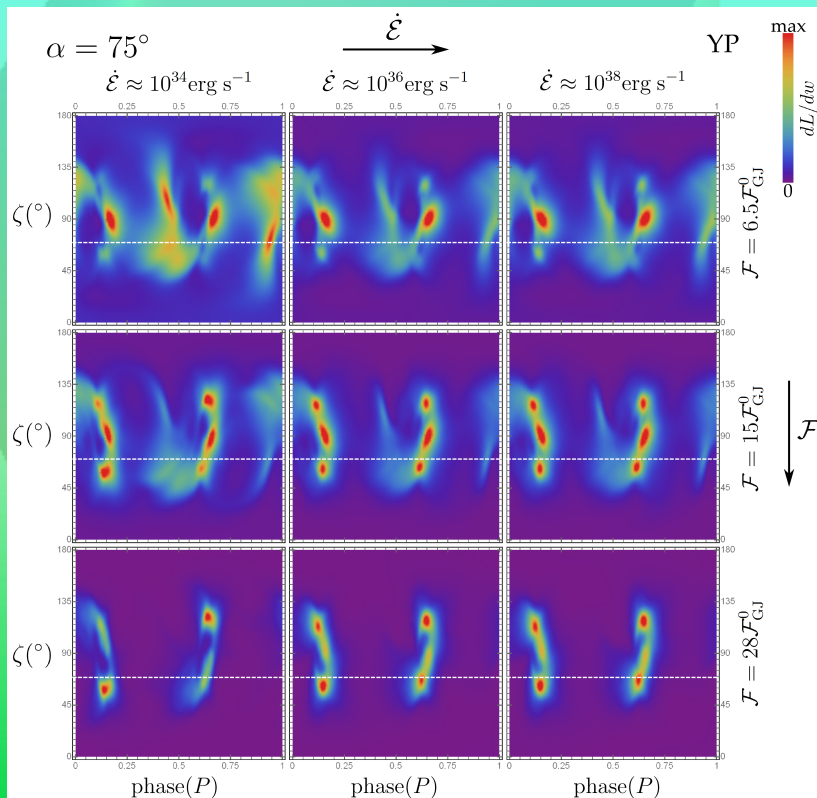
$$\mathcal{F}(\dot{\mathcal{E}})$$



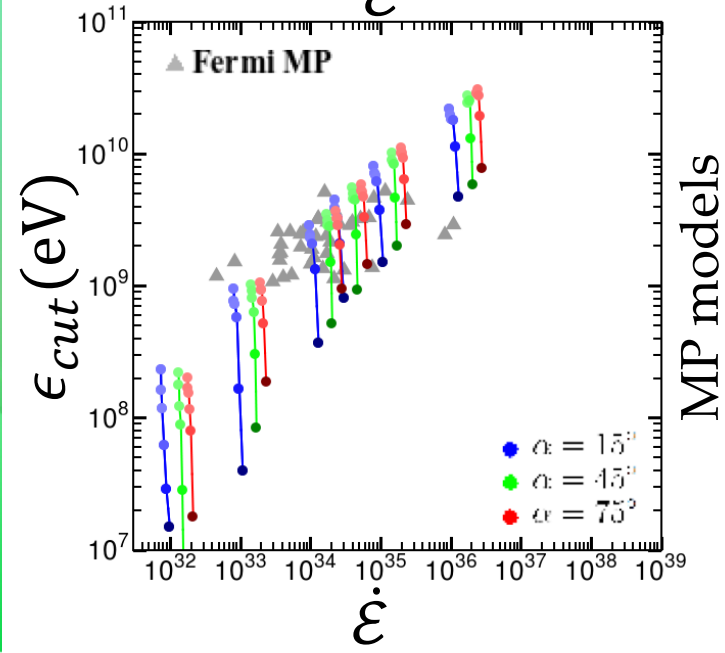
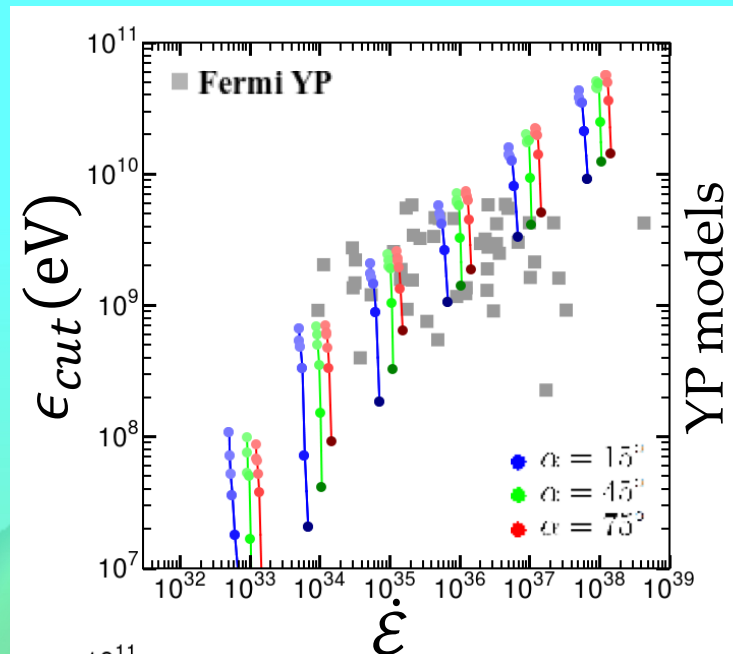
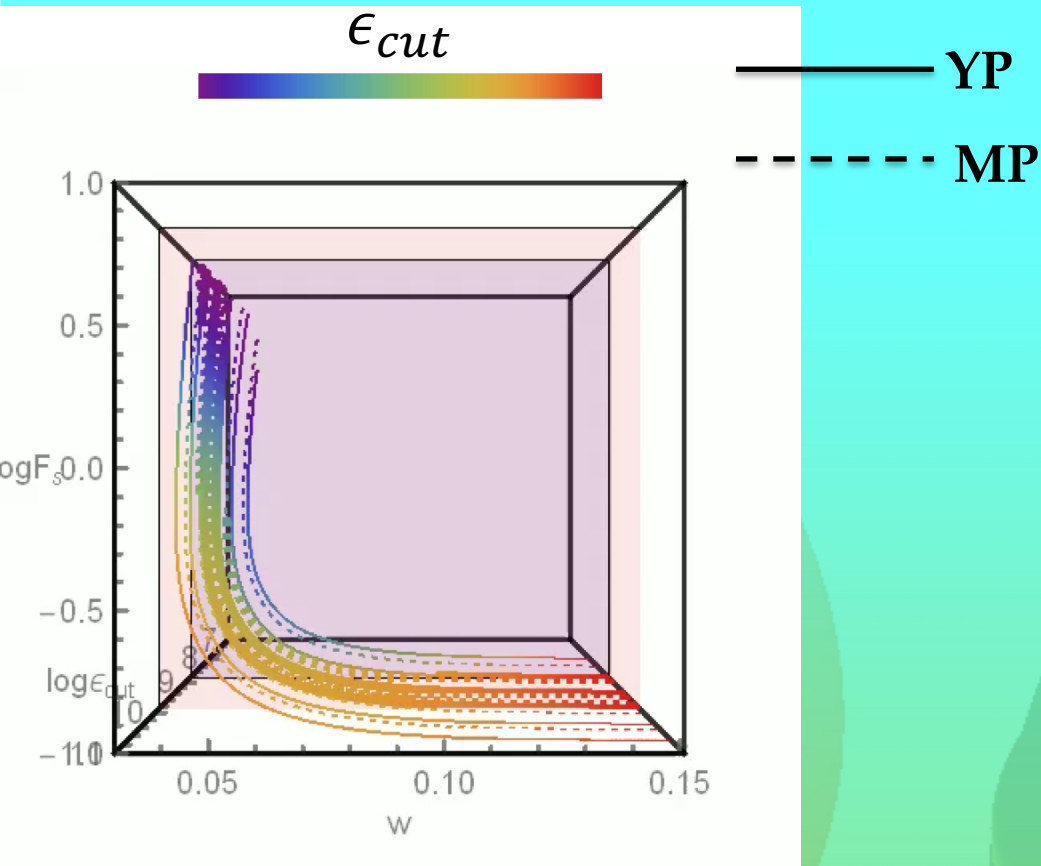
3D Kinetic Models (PIC)

But...

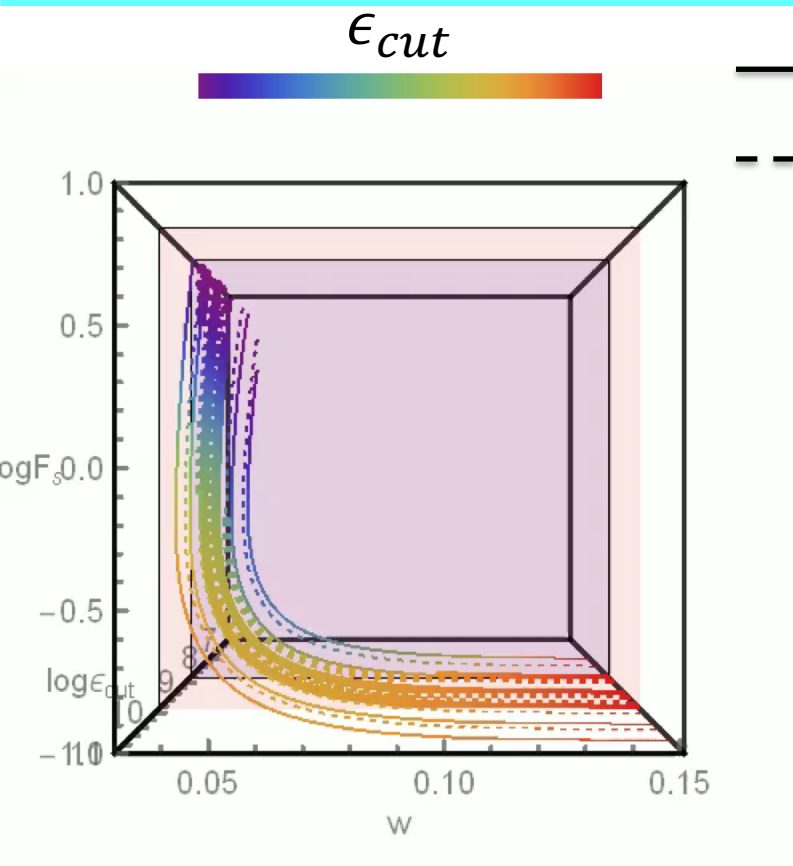
1. The γ -ray light-curves for low \mathcal{F} are messy.
2. Particle-injection regions that regulate the γ -ray emission



3D Kinetic Models (PIC)

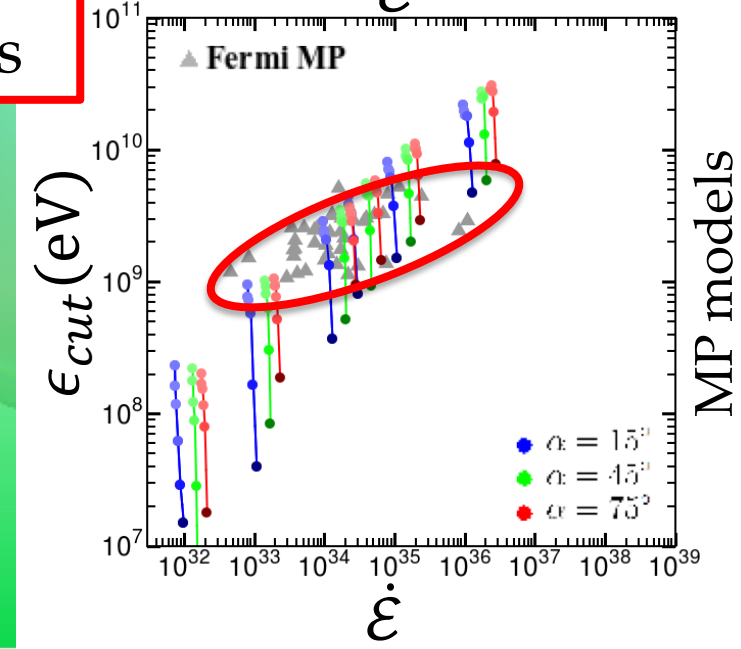
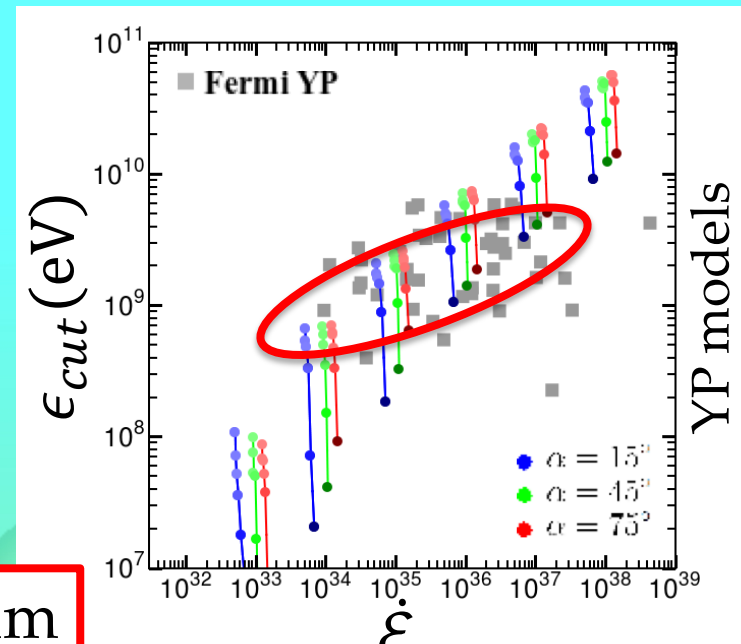


3D Kinetic Models (PIC)

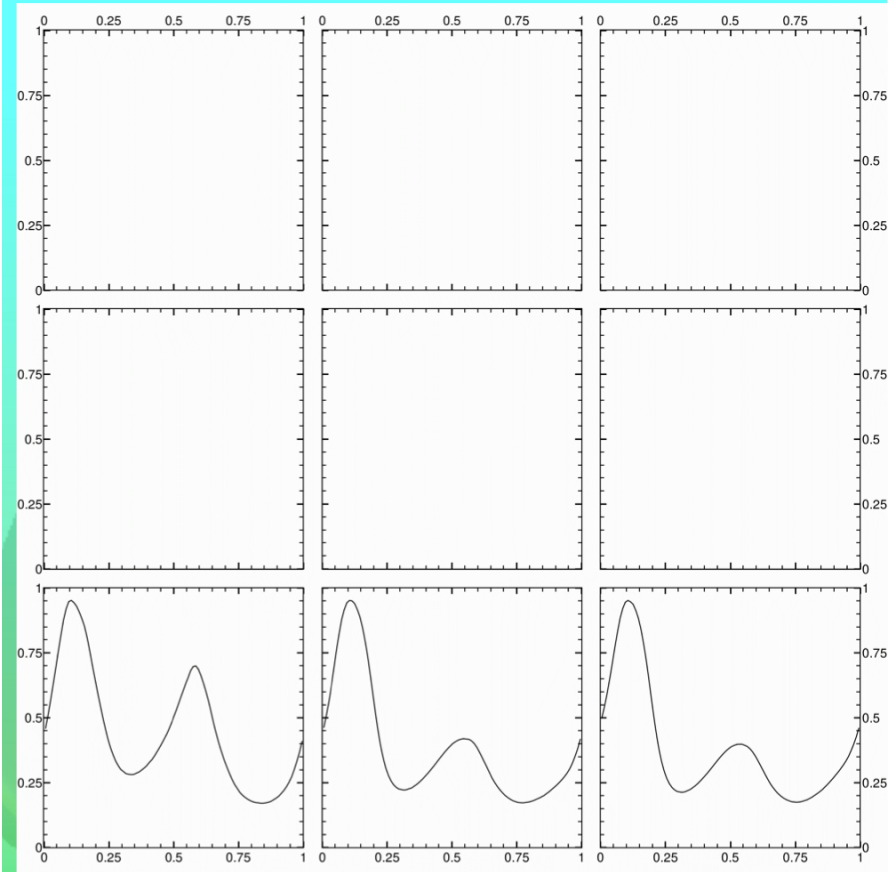
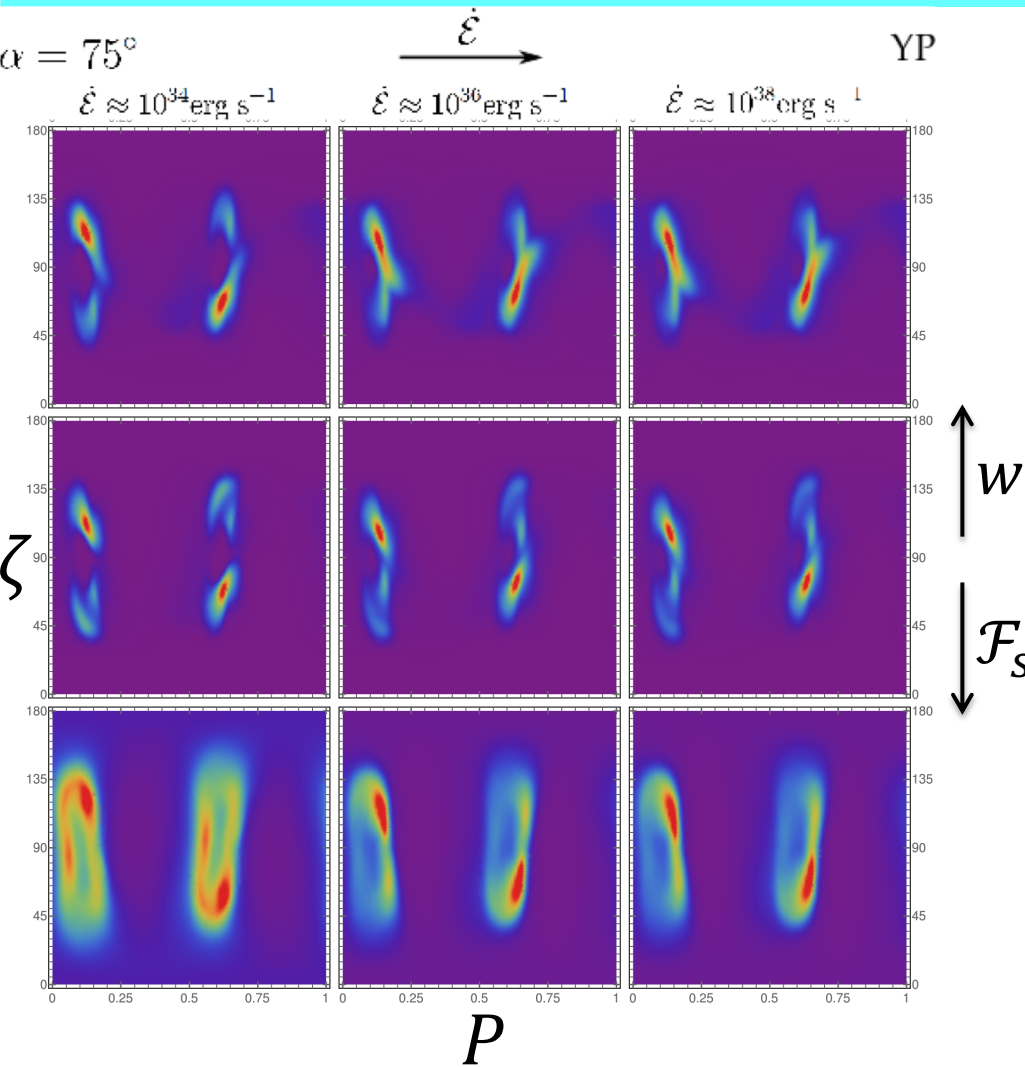


— YP
 - - - MP

Optimum models



3D Kinetic Models (PIC)



Nice, well defined light-curves similar to those observed by Fermi, for all $\dot{\mathcal{E}}$. They seem able of reproducing the $\delta - \Delta$ correlation.

Fundamental Plane

Observations & PIC Models

$$L_\gamma \propto \epsilon_{cut}^{1.18 \pm 0.24} B_*^{0.17 \pm 0.05} \dot{\xi}^{0.41 \pm 0.08}$$

Fermi data

$$L_\gamma \propto \epsilon_{cut}^{4/3} B_*^{1/6} \dot{\xi}^{5/12}$$

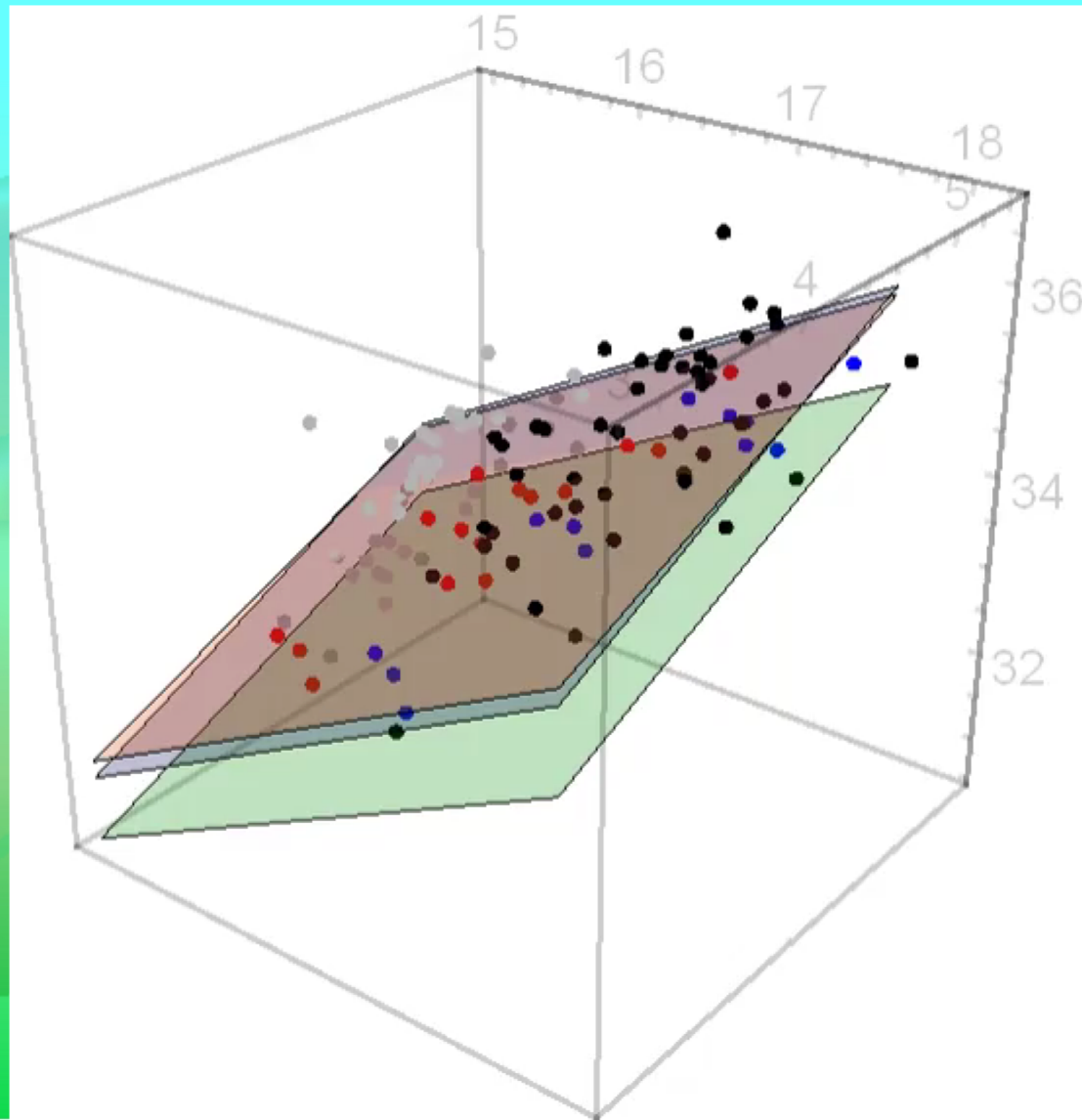
Theory CR

$$L_\gamma \propto \epsilon_{cut}^{1.56 \pm 0.34} B_*^{0.20 \pm 0.04} \dot{\xi}^{0.29 \pm 0.11}$$

PIC Models

Optimum

Fundamental Plane Observations & PIC Models



● Fermi YP

● Fermi MP

● PIC YP

● PIC MP

$$x = B_*^{1/6} \dot{\epsilon}^{5/12}$$

$$y = \epsilon_{cut}^{4/3}$$

$$z = L_\gamma$$

Fundamental Plane Observations & PIC Models

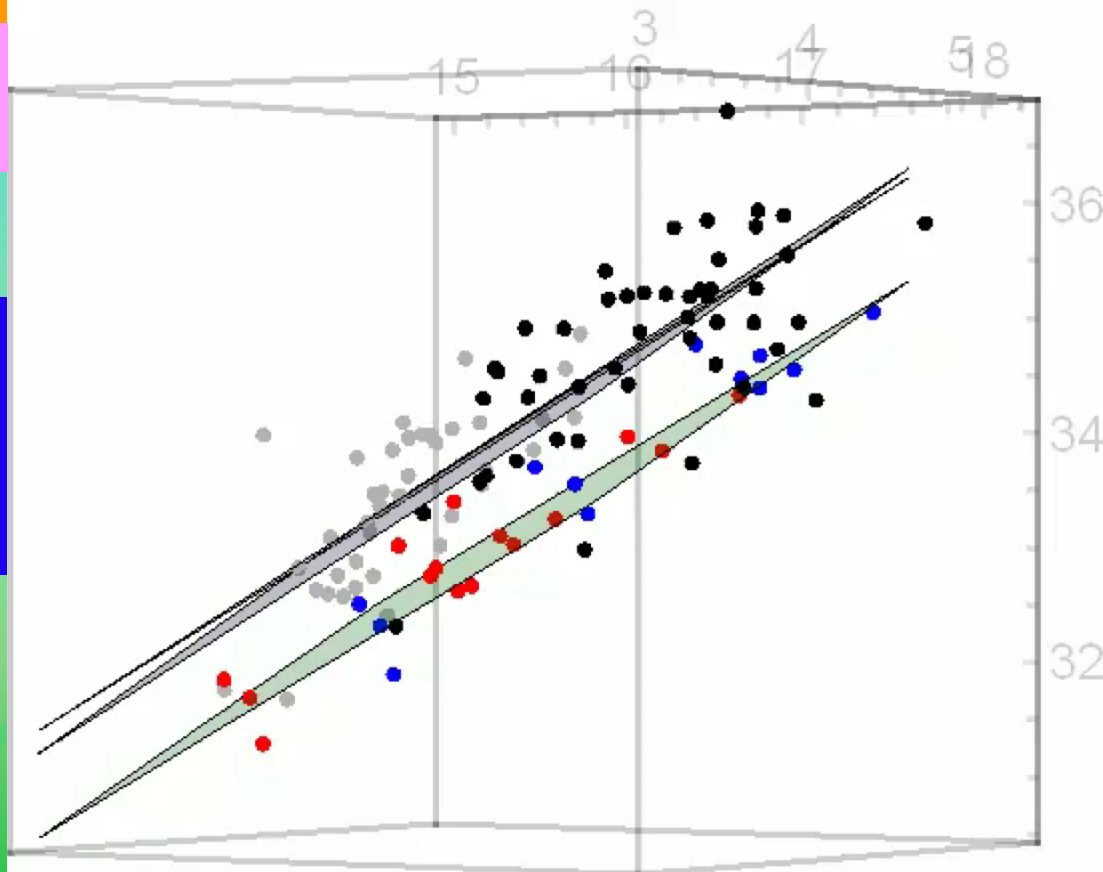
Plane distance
~0.5

Vertical distance
×5

Beaming factor f_{Ω}

Emission ($r > 2R_{LC}$)

Moment of Inertia, I



● Fermi YP
● Fermi MP

● PIC YP
● PIC MP

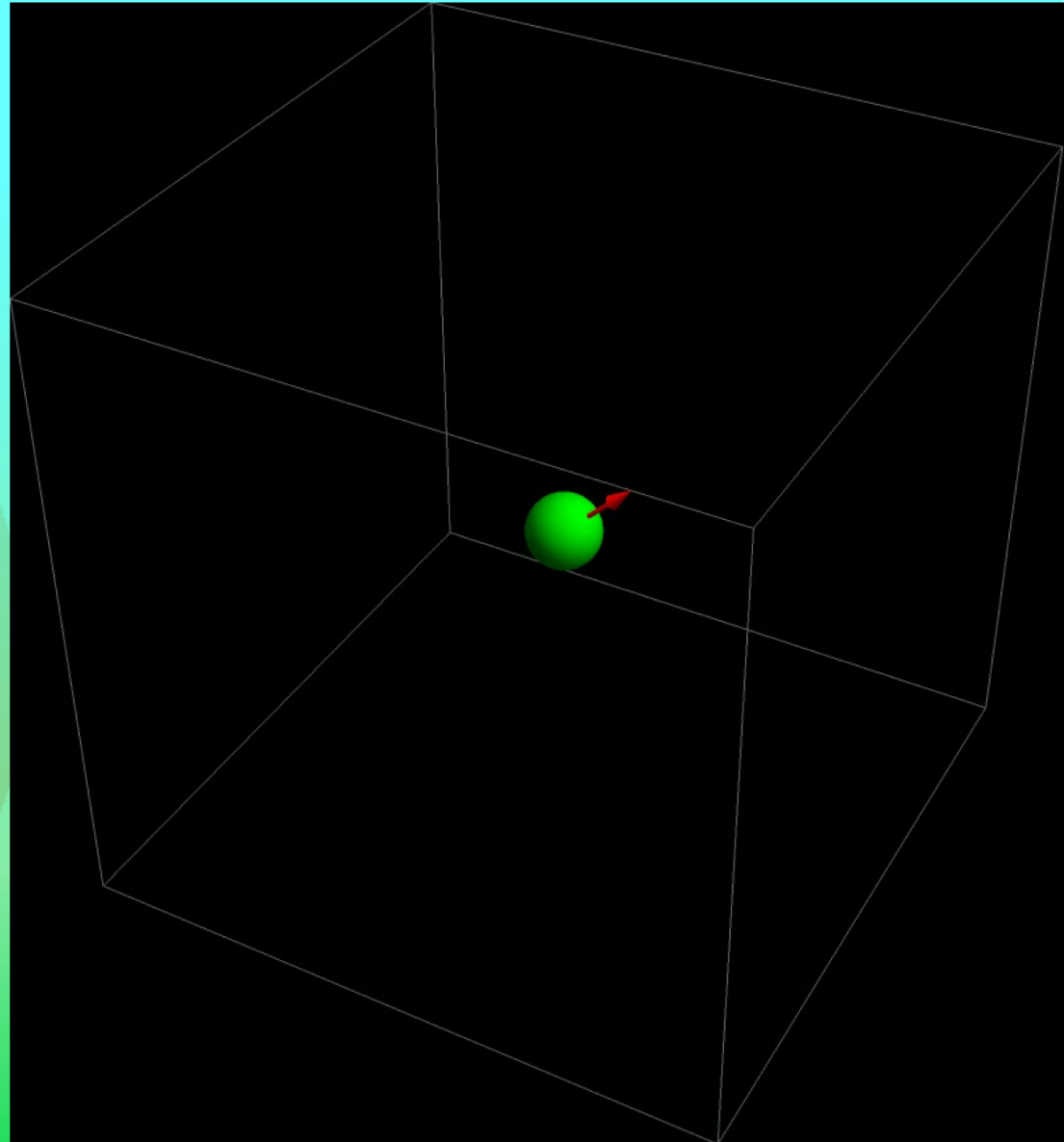
$$x = B_*^{1/6} \dot{\epsilon}^{5/12}$$
$$y = \epsilon_{cut}^{4/3}$$
$$z = L_{\gamma}$$

3D Kinetic Models (PIC)

Pulsar Theater

Particle injection
inside the LC.

Kalapothisarakos et al. (in prep.)

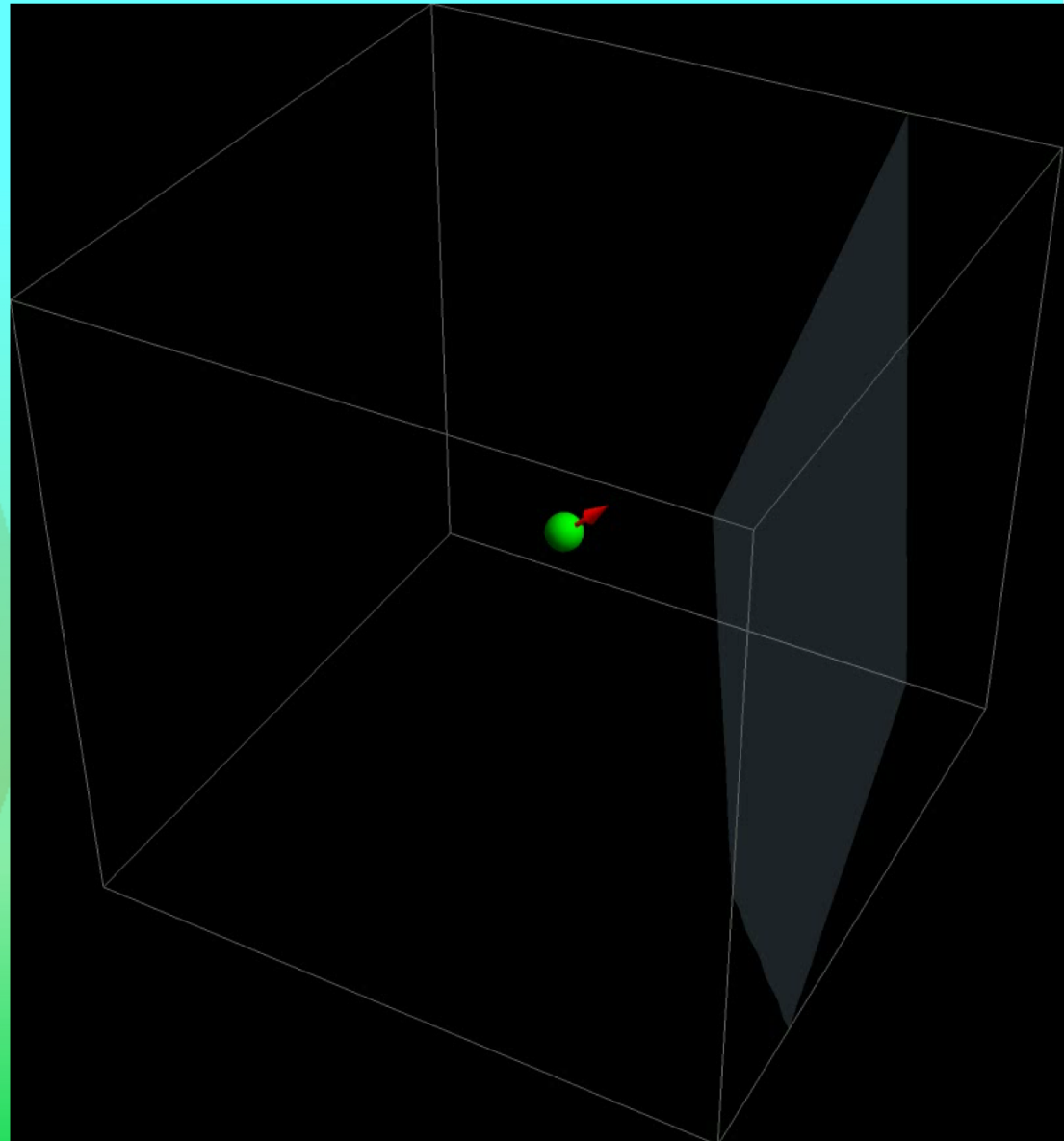
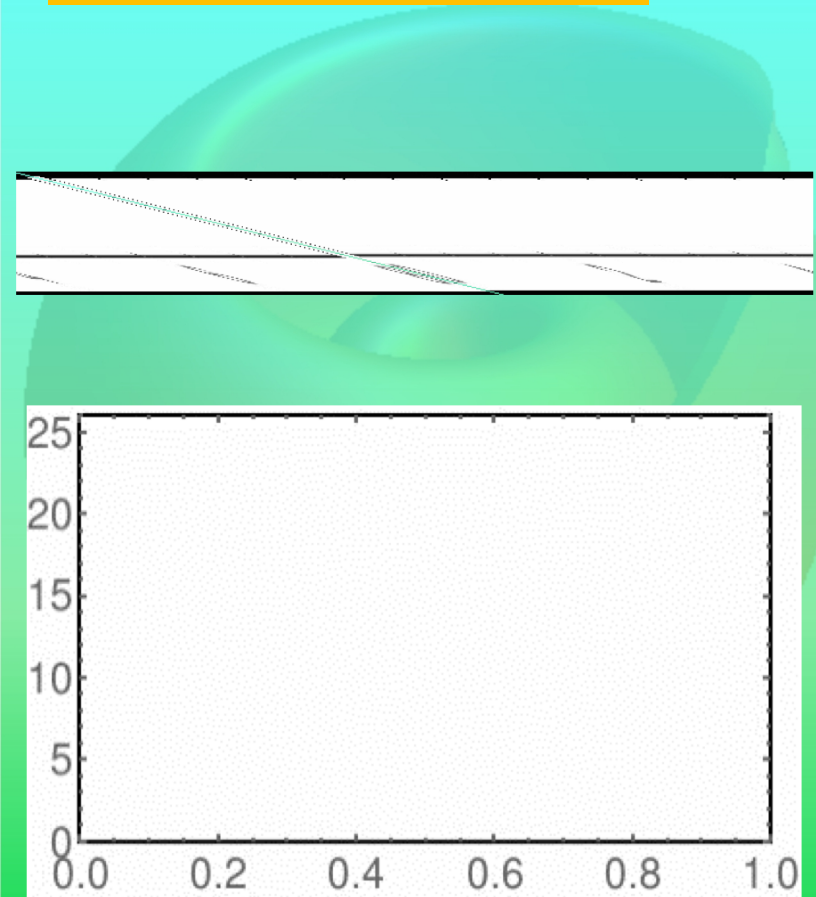


3D Kinetic Models (PIC)

Pulsar Theater

Particle injection
inside the LC.

Kalapothisarakos et al. (in prep.)



CK videos

Summary

- Fermi data contain an unprecedented level of information that uncovers the mysteries of the pulsar γ -ray emission.

Fundamental Plane

$$L_\gamma \propto \epsilon_{cut}^{1.18 \pm 0.24} B_*^{0.17 \pm 0.05} \dot{\epsilon}^{0.41 \pm 0.08} \quad \text{Fermi data}$$

$$L_\gamma \propto \epsilon_{cut}^{4/3} B_*^{1/6} \dot{\epsilon}^{5/12} \quad \text{Theory CR}$$

Separatrix Injection Model

- Kinetic PIC models indicate that the particle-injection rate, \mathcal{F}_s , in the separatrix region and the width, w , of this zone regulate the pulsar emission.

$$\sigma(\dot{\epsilon})$$

$$\mathcal{F}(\dot{\epsilon})$$

- Kinetic PIC models follow the FP. The continuation of this study is expected to provide additional constraints deepening even further our understanding.

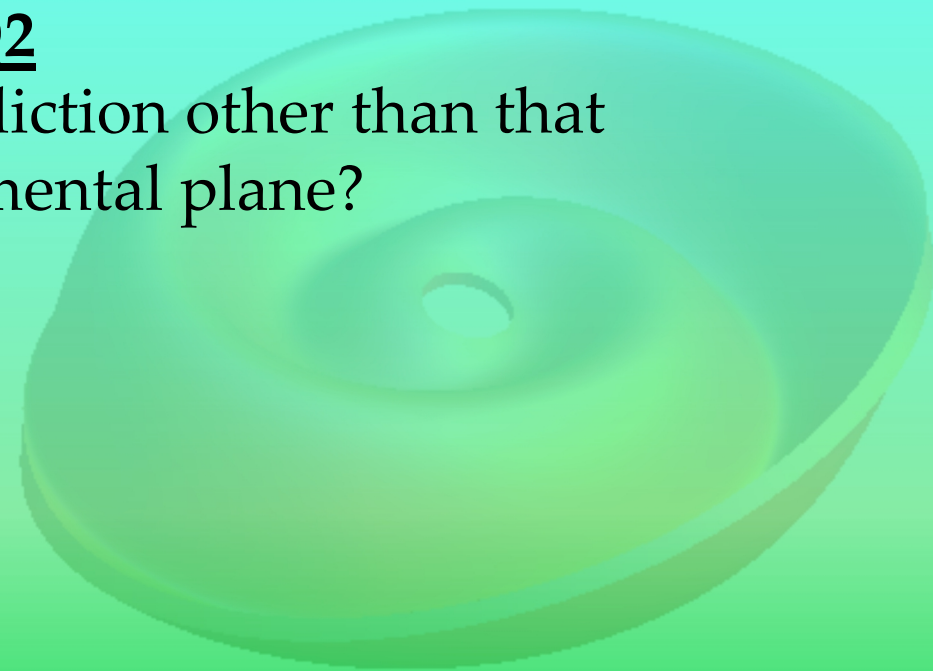
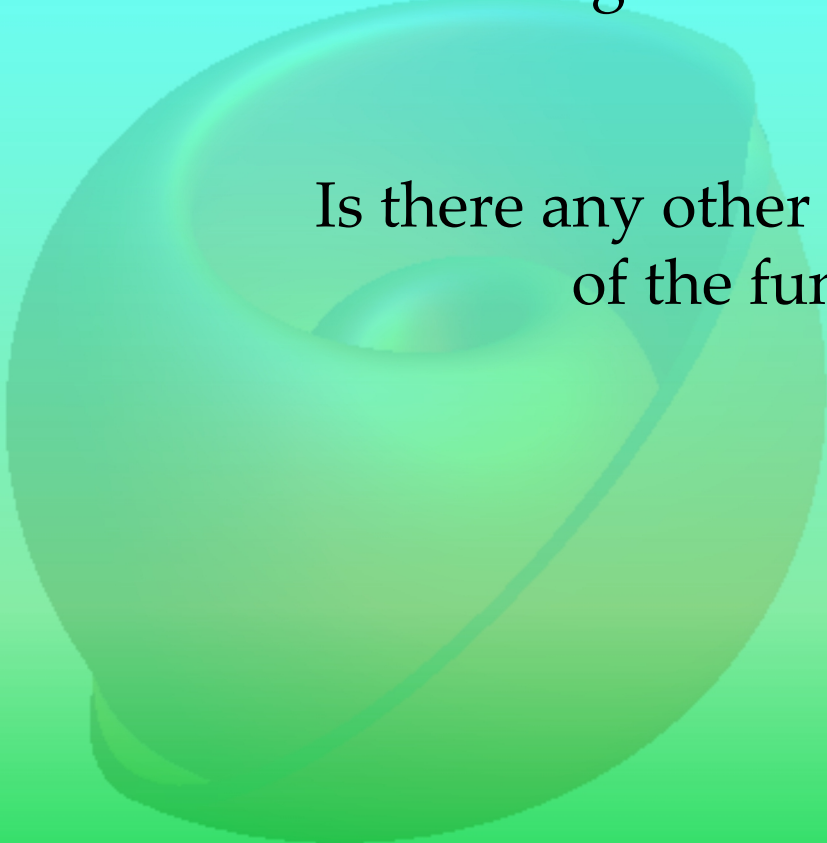
Thank you!

Q1

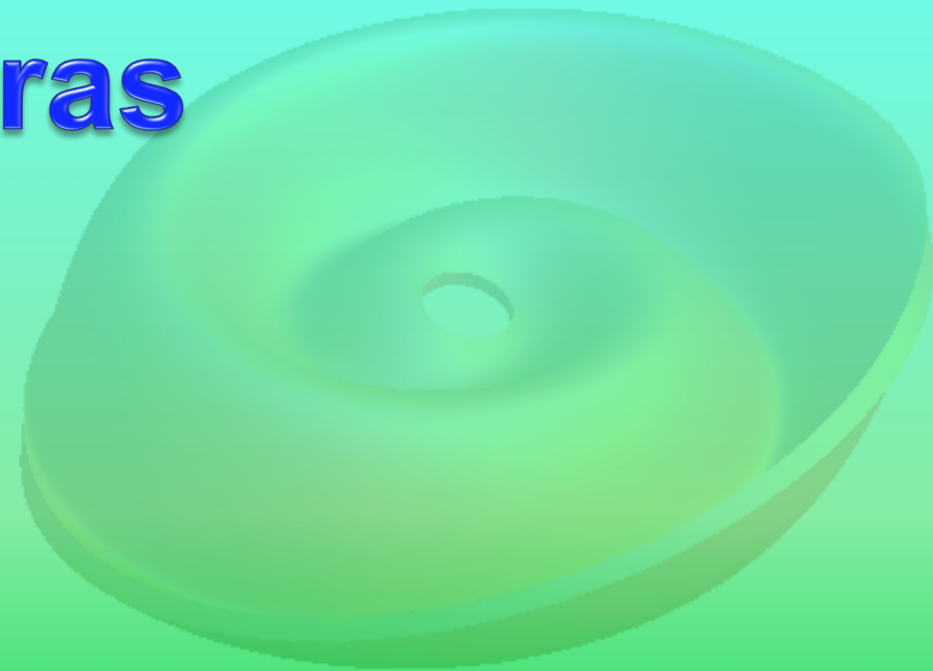
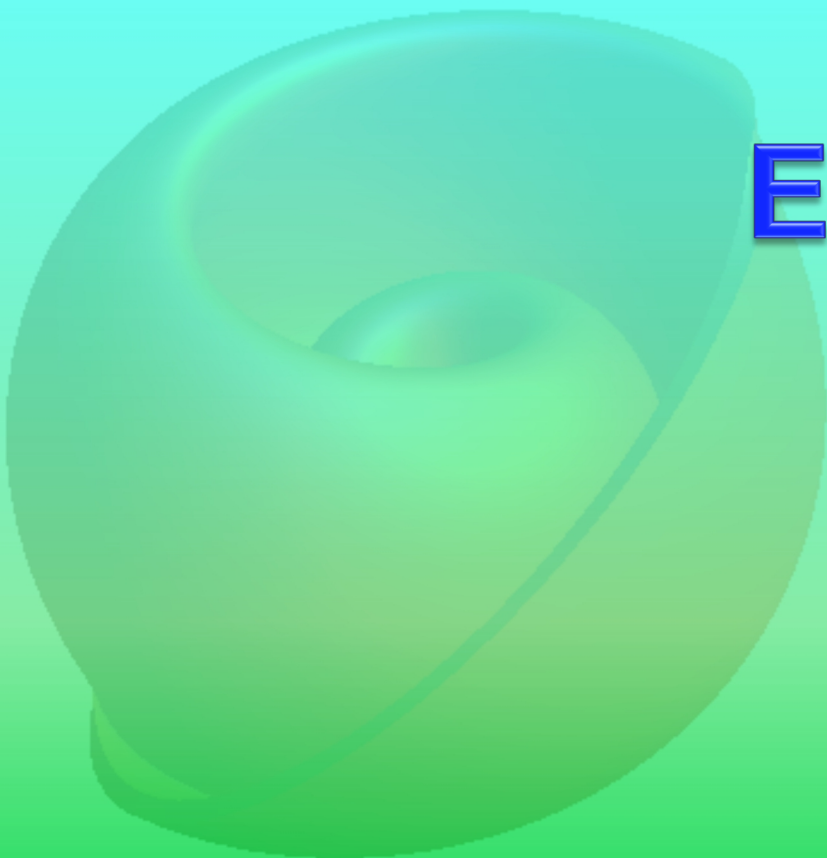
Is there any explanation about the observed scattering around the fundamental plane?

Q2

Is there any other prediction other than that of the fundamental plane?



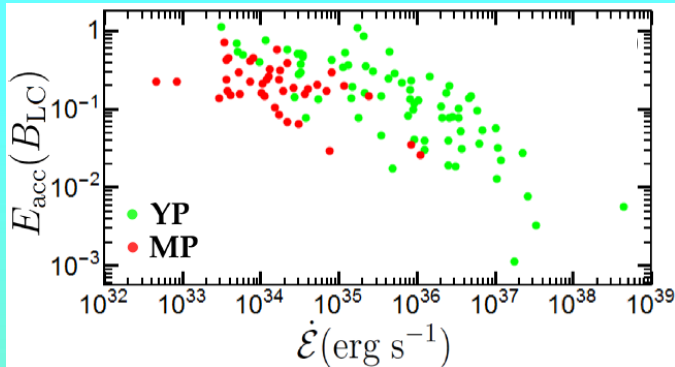
Extras



Fundamental Plane (Observations)

Is that all?

No, it is actually even better

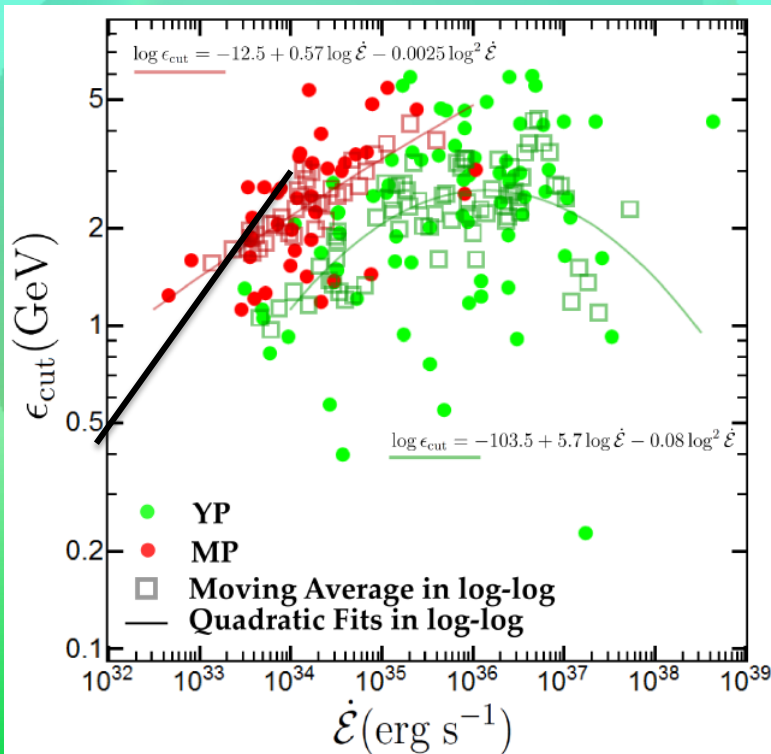


For low $\dot{\mathcal{E}}$, $E_{acc} \propto B_{LC}$

$$\epsilon_{cut} \propto B_*^{-1/8} \dot{\mathcal{E}}^{7/16}$$

$$B_{*MP} \approx 10^{-4} B_{*YP}$$

$$\epsilon_{cutMP} \approx 3\epsilon_{cutYP}$$



**Viabie interpretation
of the observed
 γ -ray pulsar death-line**

Better sensitivity in the
MeV-band telescope (AMEGO)

VHE pulsed detections

$$N_p \rightarrow \times 30$$

$$N_p > 230 \text{ (117 in 2PC; Abdo et al. 2013)}$$

Recent detections by *MAGIC* and *HESSII* of very high energy (VHE) emission from the **Crab** (Ansoldi et al. 2016), **Vela** (Djannati-Atai et al. 2017), and **Geminga** (Lopez et al. 2018) pulsars imply an additional emission component, and inverse Compton (IC) seems to be the most reasonable candidate (Rudak & Dyks 2017; Harding et al. 2018).

In any case, the multi-TeV photon energies detected imply very high particle energies ($\gamma_L > 10^7$).

3D Kinetic Models (PIC)

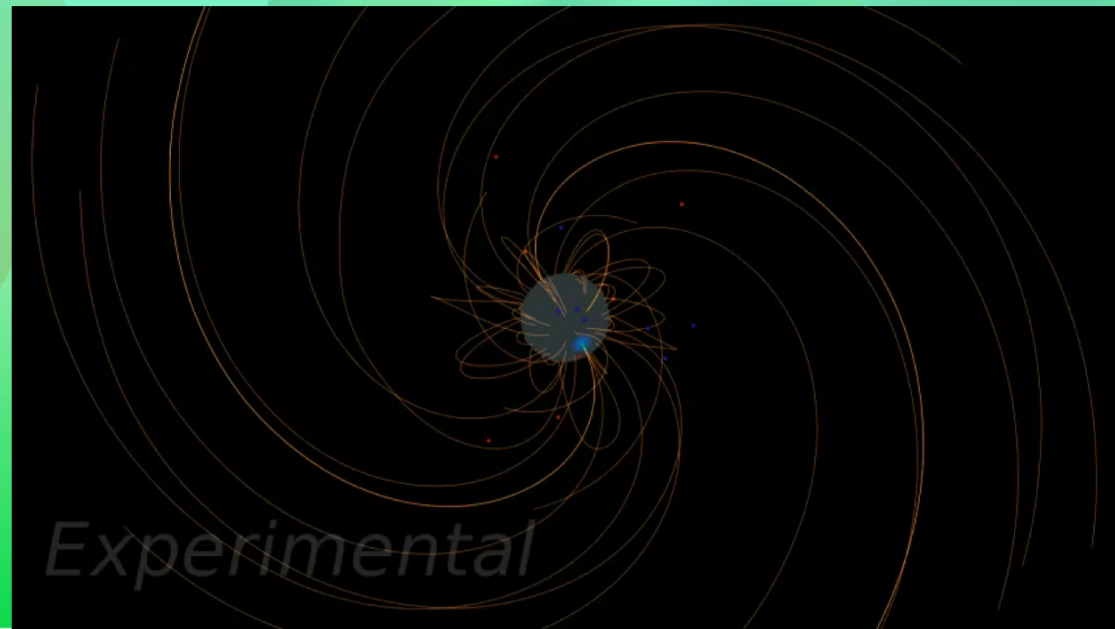
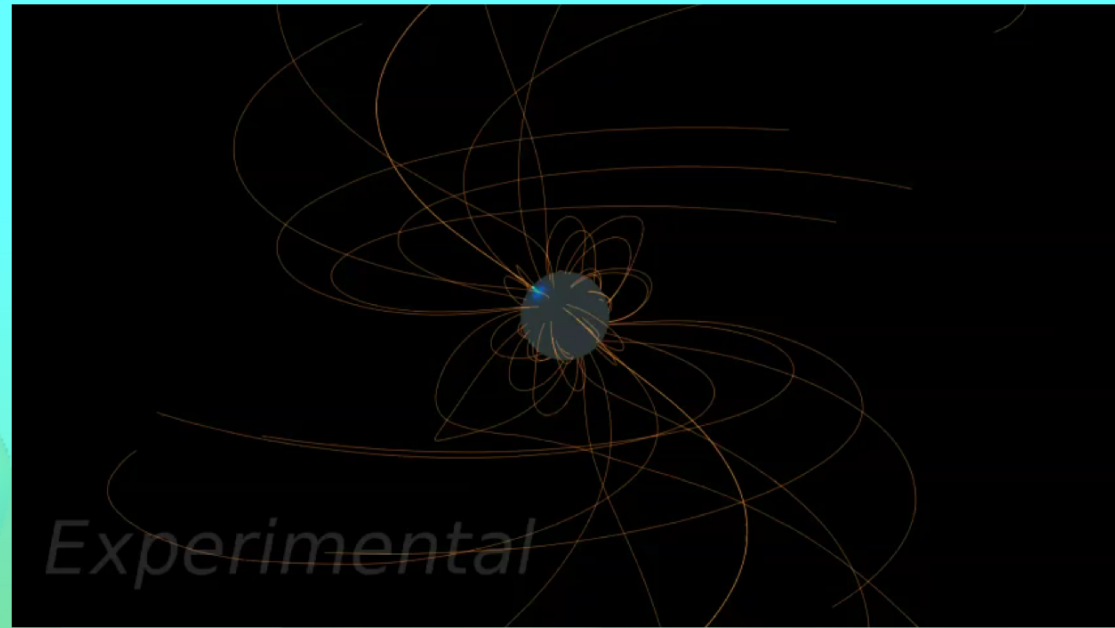
Pulsar Theater

Particle injection near
the stellar surface.

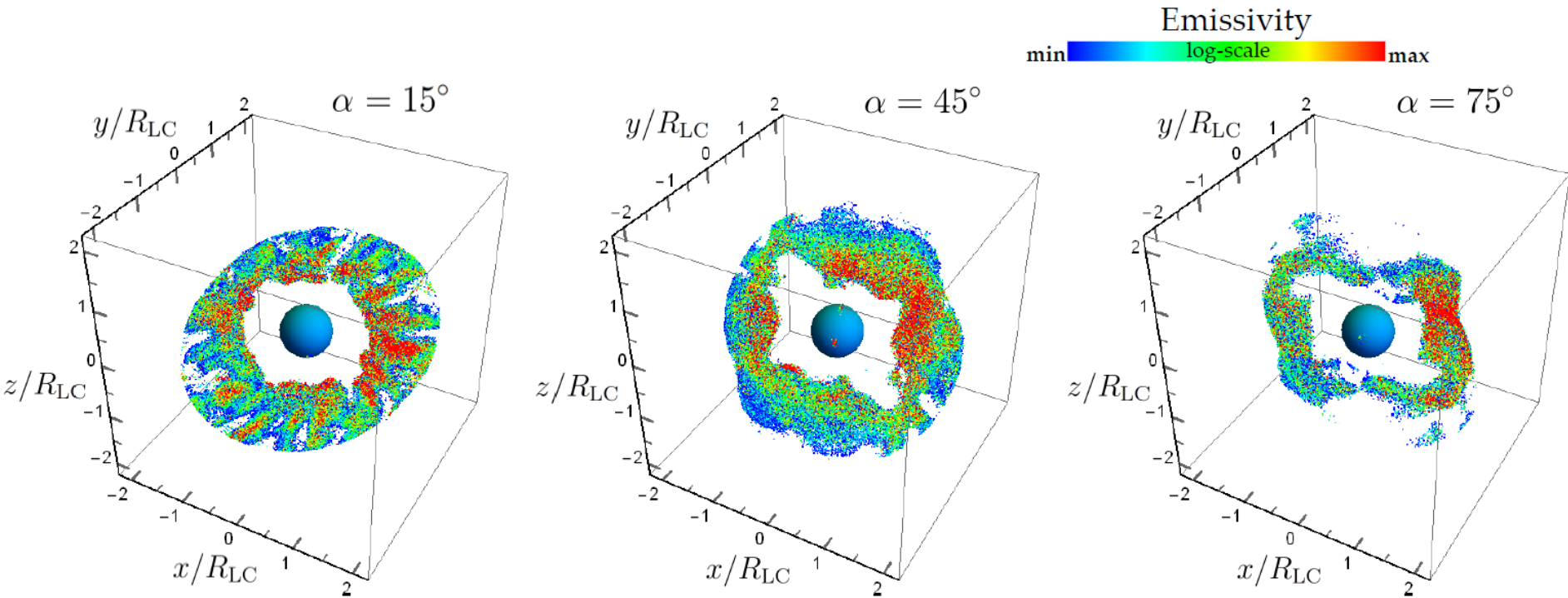
Brambilla et al. 2018

● e^-
● e^+

NASA/GSFC videos



3D Kinetic Models (PIC)



- 95% of the total emission
- Near the equatorial current sheet
- For low α -values closer to the Y-point (LC)
- For high α -values closer to the rotational equator compared to the theoretical extend of the ECS

Fundamental Plane (Observations)

88 Fermi YPs+MPs

$$L_{\gamma(3D)} = 10^{14.2 \pm 2.3} \epsilon_{cut}^{1.18 \pm 0.24} B_*^{0.17 \pm 0.05} \dot{\xi}^{0.41 \pm 0.08}$$

ϵ_{cut} (MeV), B_* (G), L_{γ} , $\dot{\xi}$ (erg/s)

Kalapotharakos et al. (2019)

Fermi data

$$L_{\gamma} \propto \epsilon_{cut}^{4/3} B_*^{1/6} \dot{\xi}^{5/12}$$

Theory CR

B_* : 4 OoM

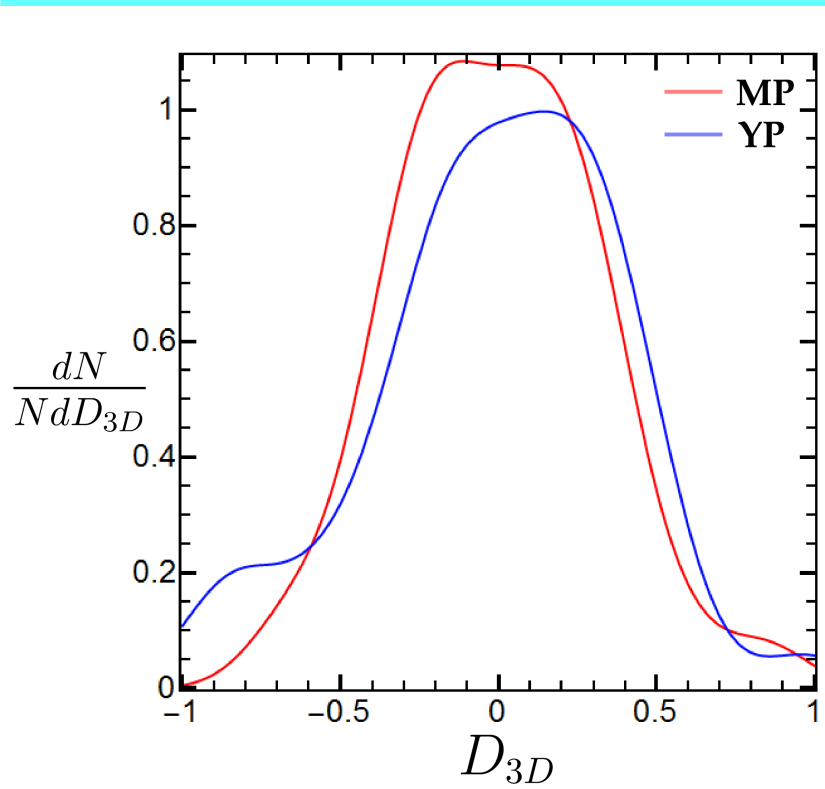
$\dot{\xi}$: 6 OoM

L_{γ} : 6 OoM

ϵ_{cut} : < 1 OoM

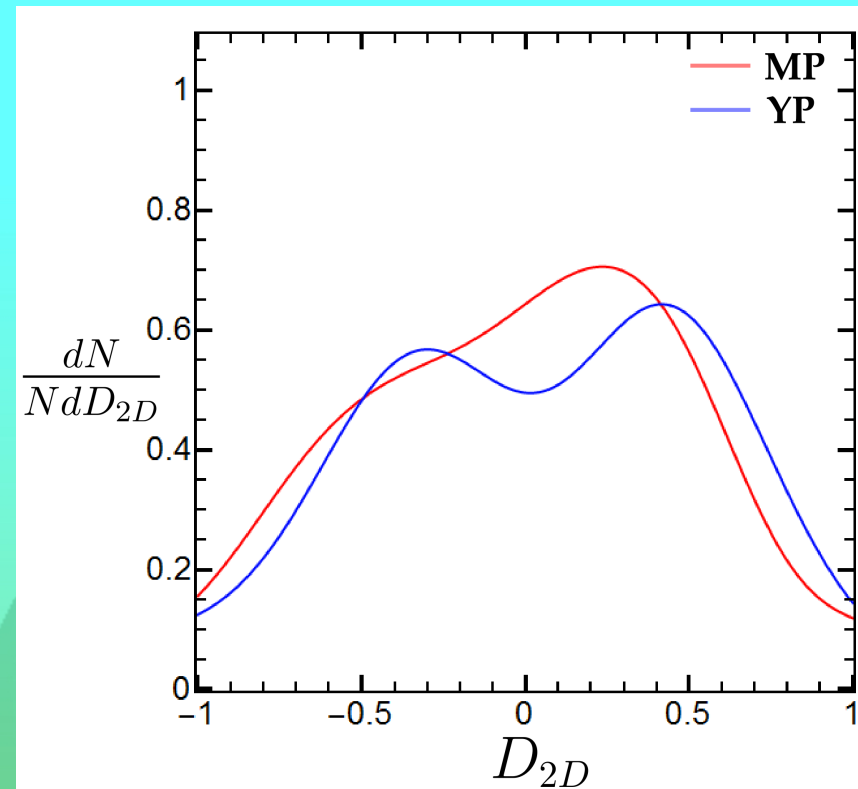
$$L_{\gamma(2D)} = 10^{15.0 \pm 2.6} B_*^{0.11 \pm 0.05} \dot{\xi}^{0.51 \pm 0.09}$$

Fundamental Plane (Observations)



$$AIC_{3D} = 159$$

$$BIC_{3D} = 172$$

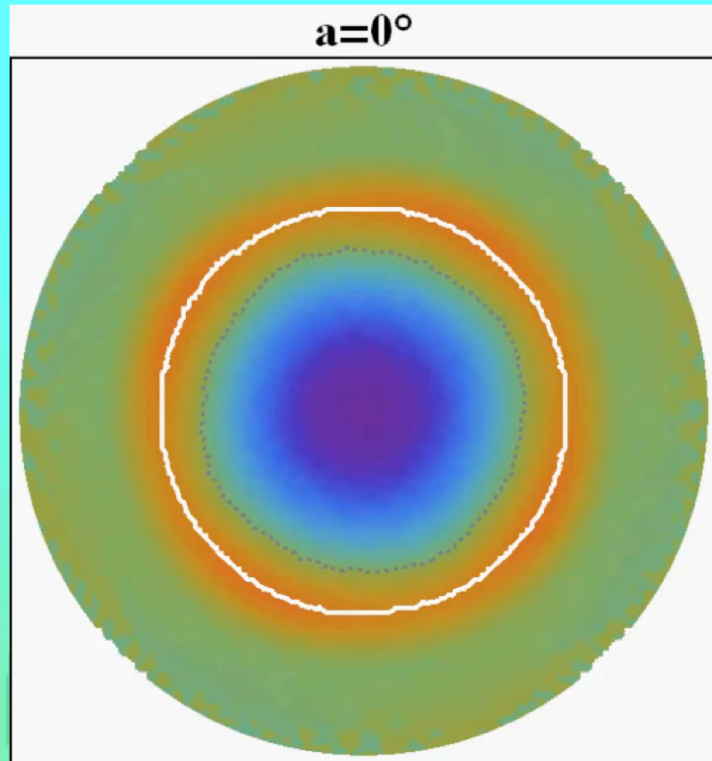


$$AIC_{2D} = 180$$

$$BIC_{2D} = 189$$

3D Kinetic Models (PIC)

Separatrix injection model



The γ -ray pulsar radiation is mainly regulated by

1. The particle injection rate \mathcal{F}_s along the separatrix
2. The width w of the separatrix zone

Kalapothisarakos et al. (in prep)

Requirements

The particle injection rate along the open and the closed field-lines is not very small.

$$(> 5\mathcal{F}_{GJ}^0)$$

However, it is not necessary to be high.

$$(< 10\mathcal{F}_{GJ}^0)$$

3D Kinetic Models (PIC)

Separatrix injection model

The γ -ray pulsar radiation is mainly regulated by

1. The particle injection rate \mathcal{F}_s along the separatrix
2. The width w of the separatrix zone

Kalapothisarakos et al. (in prep)

Requirements

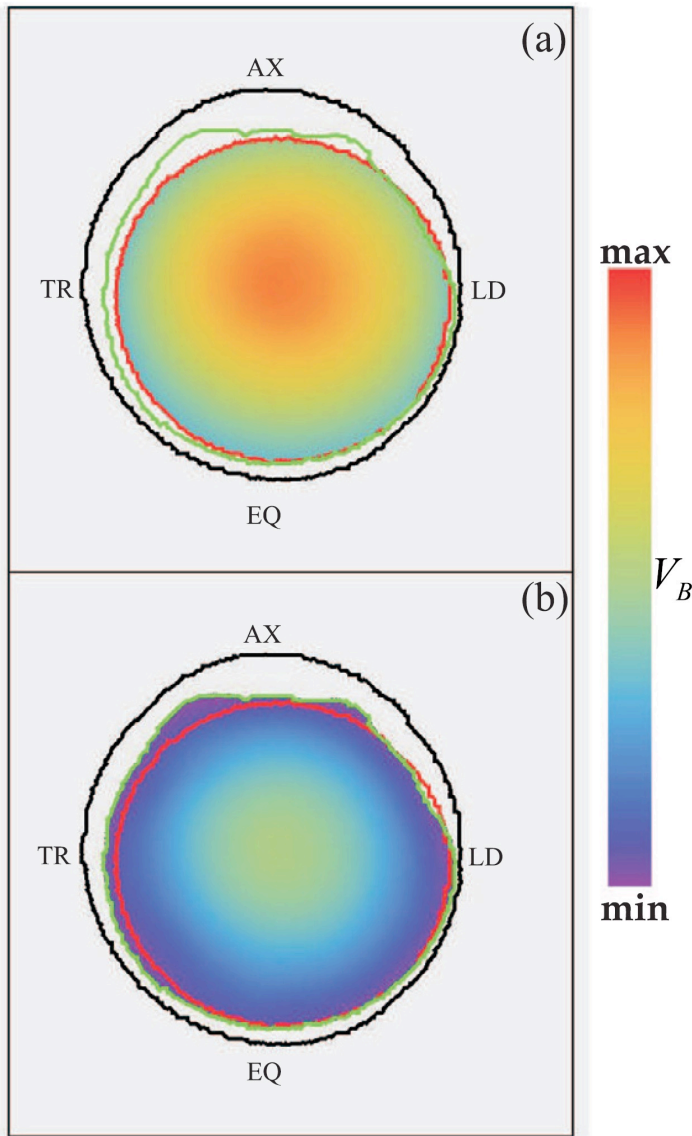
The particle injection rate along the open and the closed field-lines is not very small.

$$(> 5\mathcal{F}_{GJ}^0)$$

However, it is not necessary to be high.

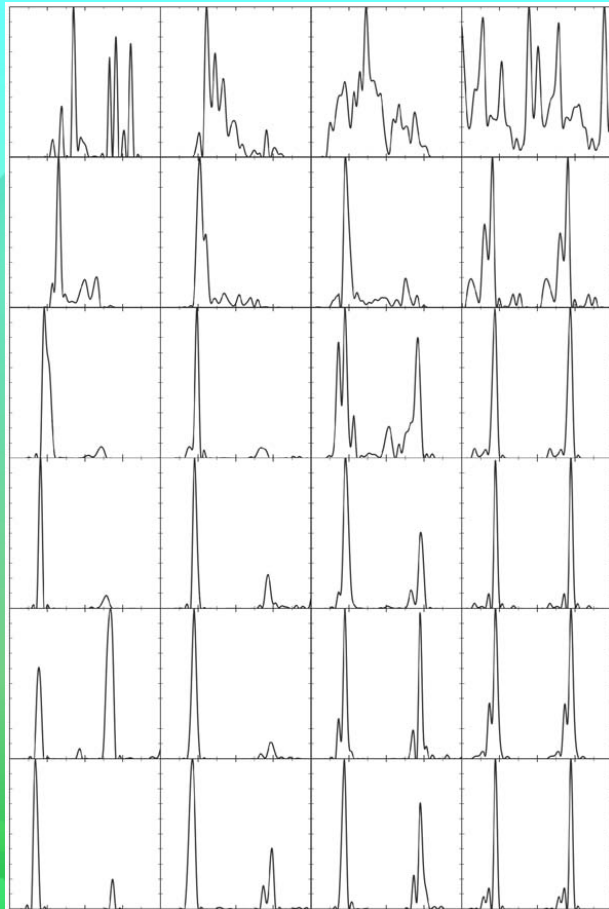
$$(< 10\mathcal{F}_{GJ}^0)$$

$a = 15^\circ$ $\sigma = 0.02\Omega$

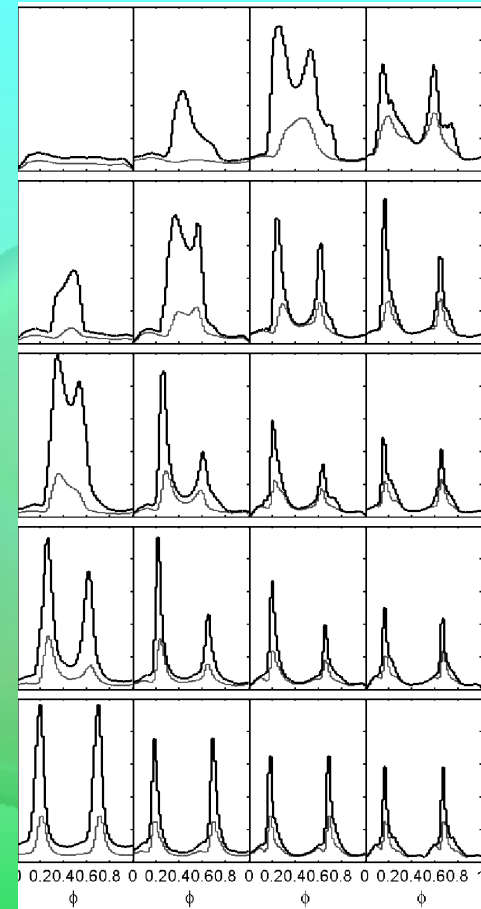


FFE Models

γ -ray light-curves from the region near the equatorial current sheet (ECS)

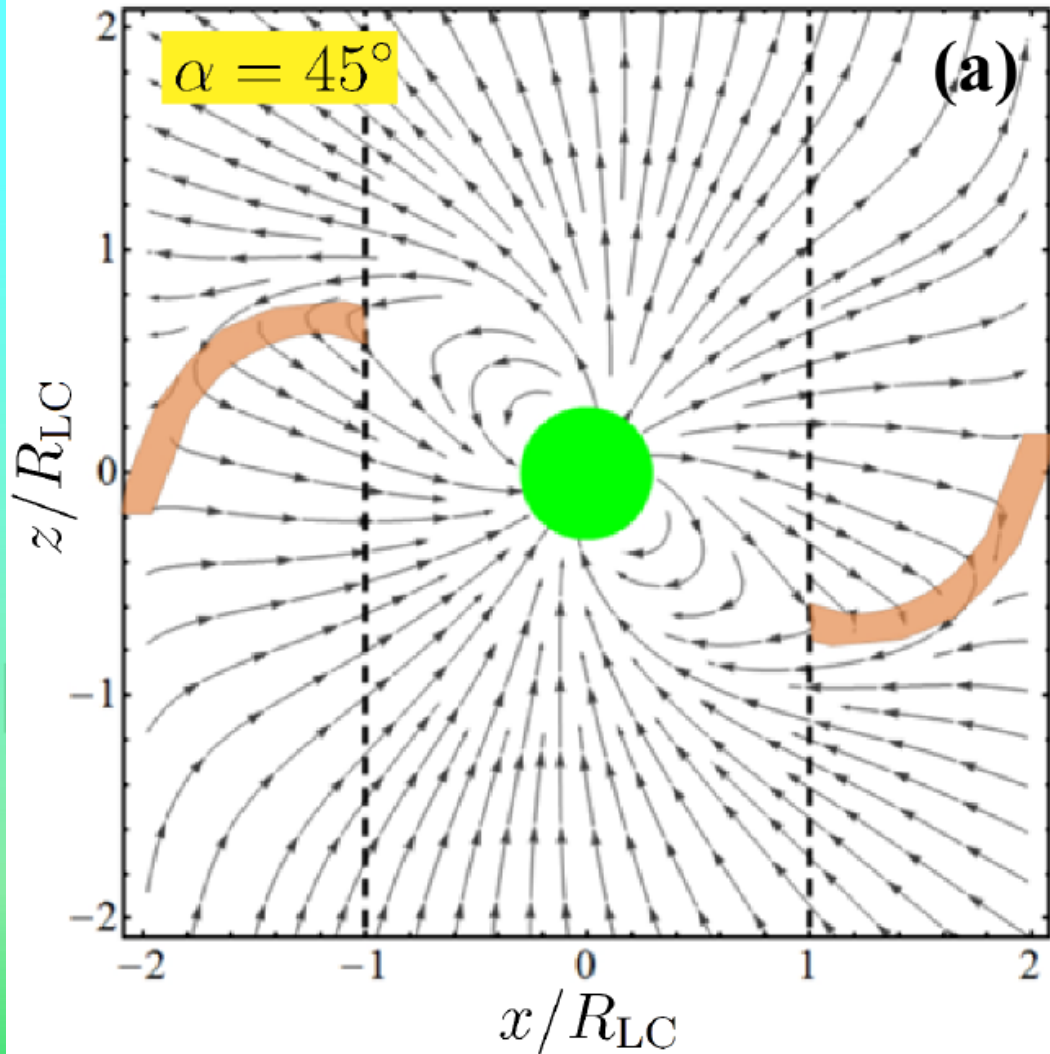


Contopoulos & Kalapotharakos (2010)



Bai & Spitkovsky (2010)

FIDO Models

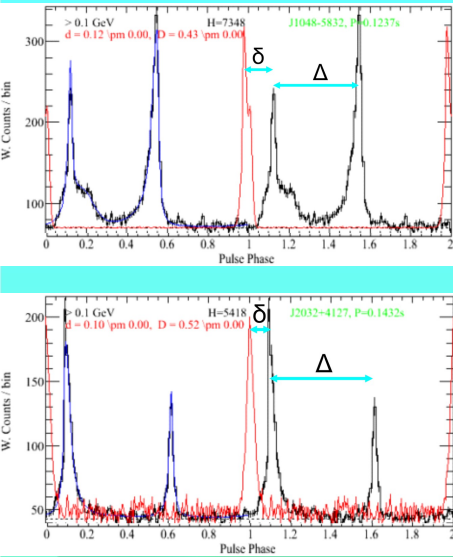


FIDO Models
(FFE Inside the Light-Cylinder,
Dissipative Outside the Light
Cylinder)

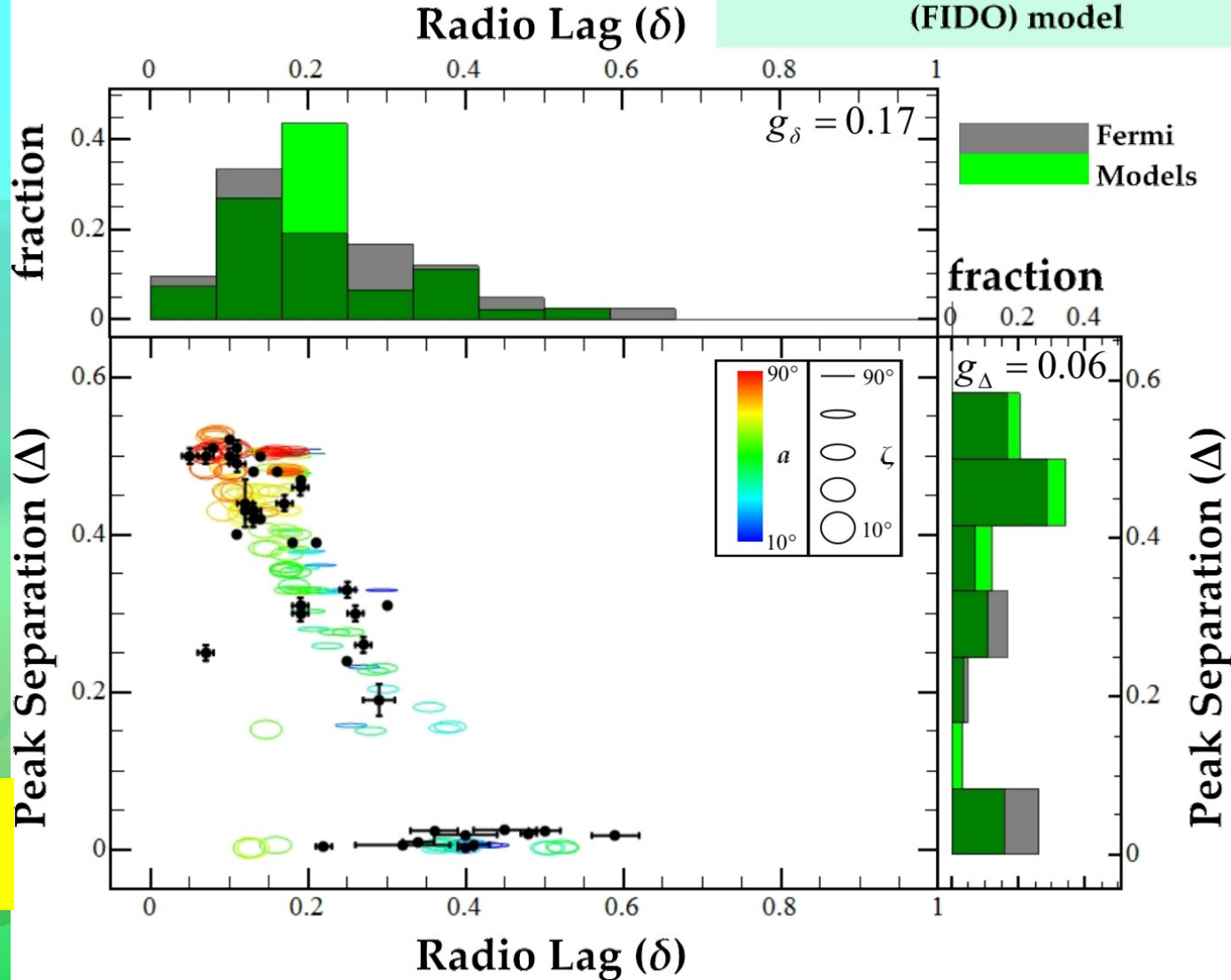
σ : conductivity

Kalapocharakos et al. (2014, 2017)

FIDO Models



FFE Inside Dissipative Outside (FIDO) model



radio-lag (δ)
vs
peak-separation (Δ)

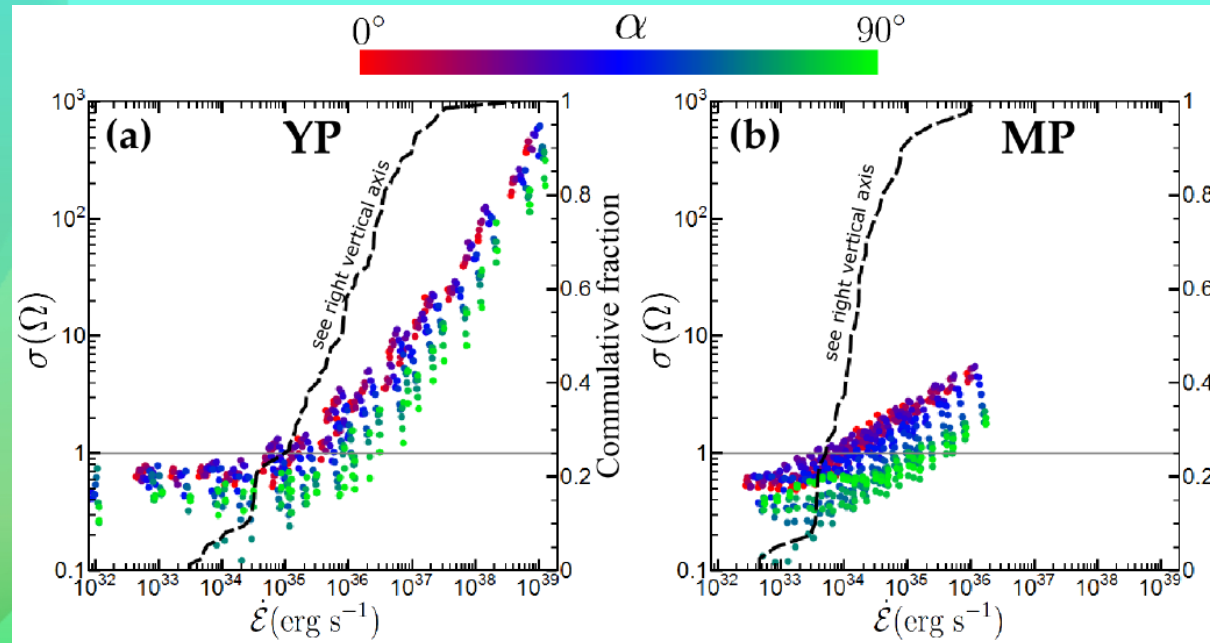
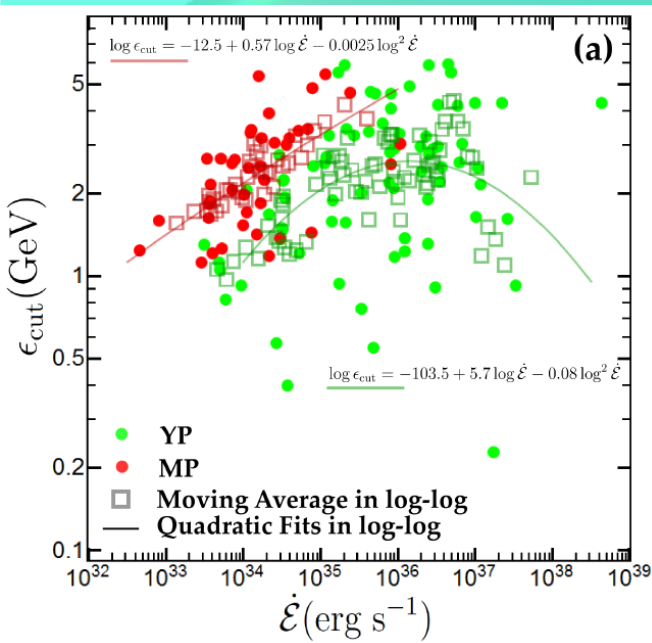
Test particles
Curvature Radiation

Kalapothisarakos et al. (2014)

FIDO Models

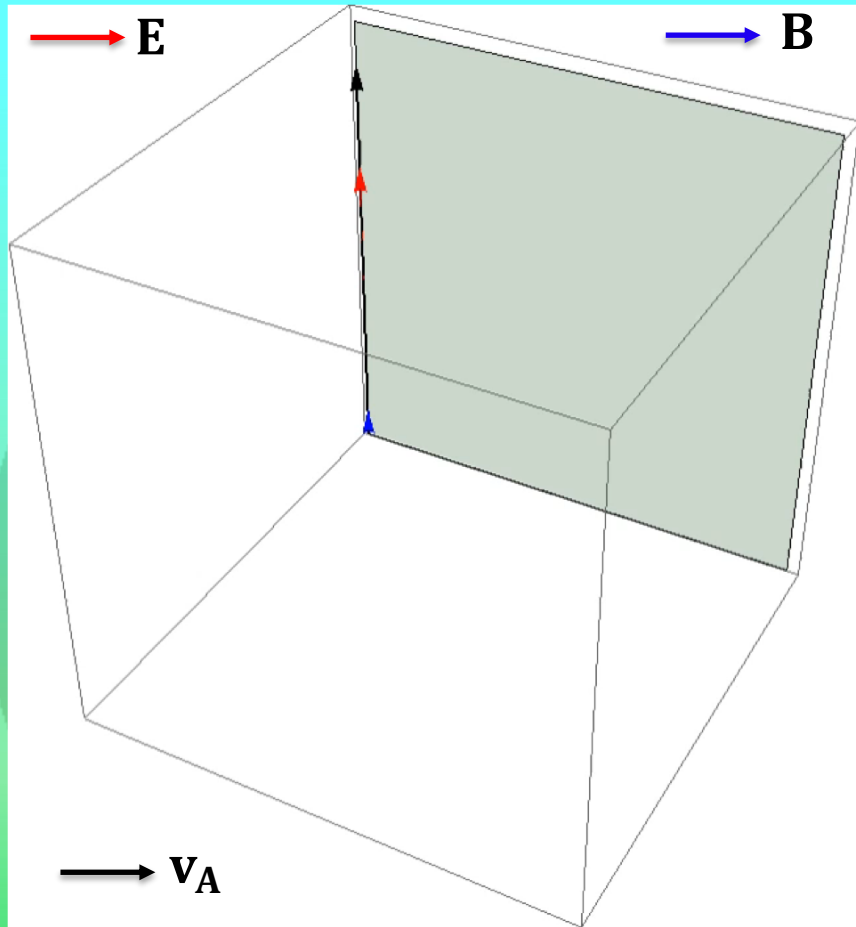
The FIDO model allows the calculation of the phase-averaged, phase-resolved spectra and the calculation of the total γ -ray luminosity.

$$\sigma(\dot{\epsilon})$$



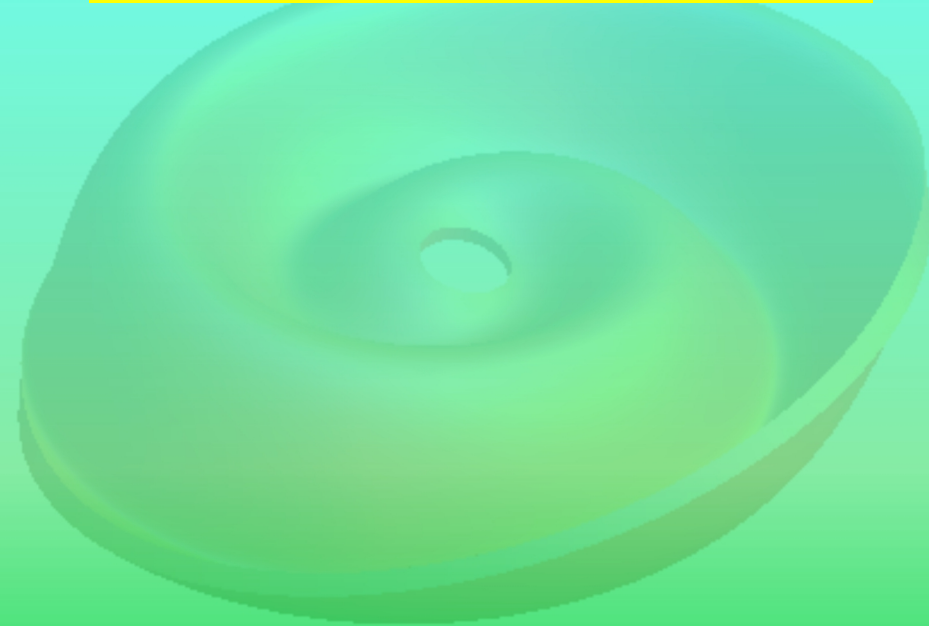
Kalopotharakos et al. (2017)

Orbital Exploration (SR↔CR)



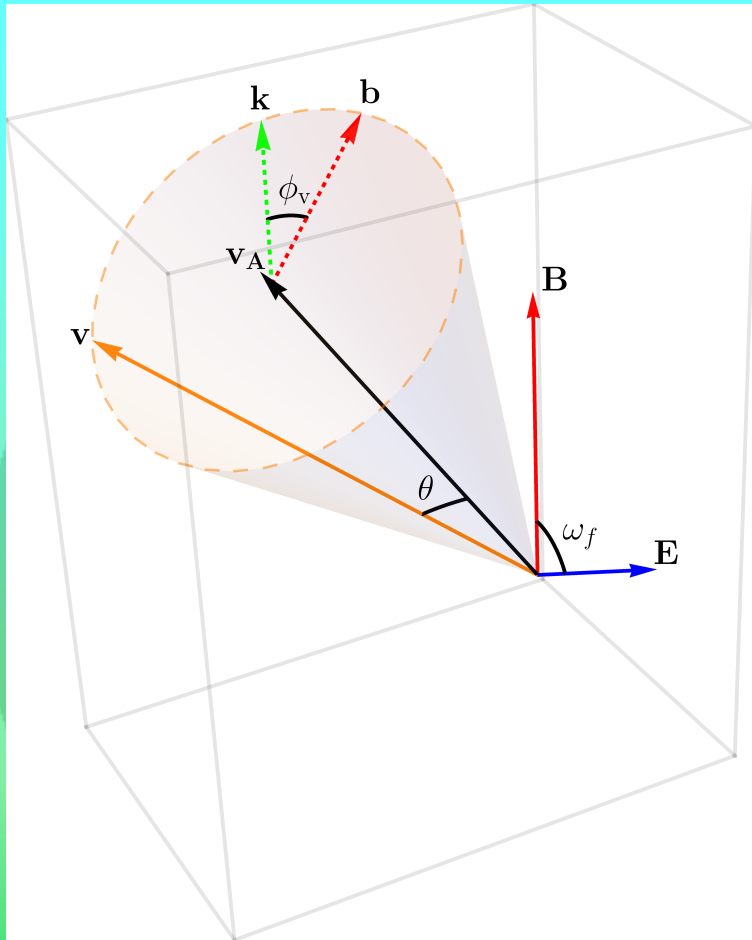
$$\mathbf{v}_A = \frac{\mathbf{E} \times \mathbf{B} \pm (E_0 \mathbf{E} + B_0 \mathbf{B})}{E_0^2 + B^2}$$

Aristotelian Electrodynamics
(Gruzinov 2012; Kelner et al. 2015)



Kalapocharakos et al. (2019)

Orbital Exploration (SR \leftrightarrow CR)



Kalapothisarakos et al. (2019)

$$\mathbf{v}_A = \frac{\mathbf{E} \times \mathbf{B} \pm (\mathbf{E}_0 \mathbf{E} + \mathbf{B}_0 \mathbf{B})}{E_0^2 + B^2}$$

Aristotelian Electrodynamics
(Gruzinov 2012; Kelner et al. 2015)

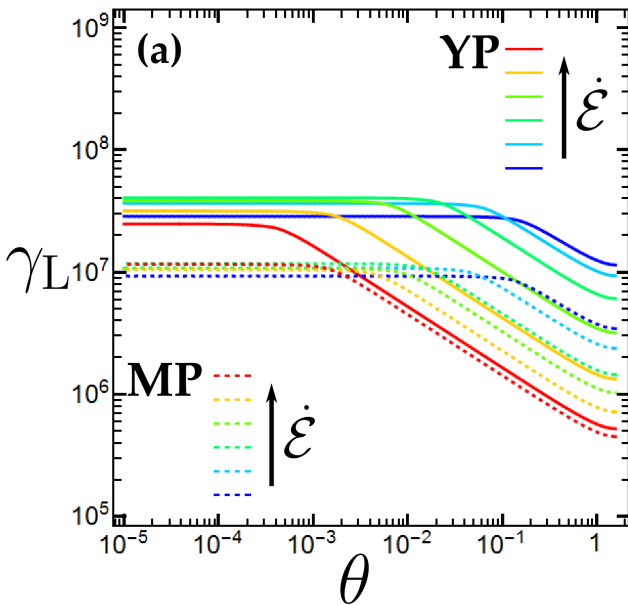
$$R_C = \frac{\gamma_L m_e c^2}{q_e B_{eff}}$$

$$B_{eff} = \sqrt{\left(\mathbf{E} + \frac{\mathbf{v} \times \mathbf{B}}{c}\right)^2 - \left(\frac{\mathbf{v} \cdot \mathbf{B}}{c}\right)^2}$$

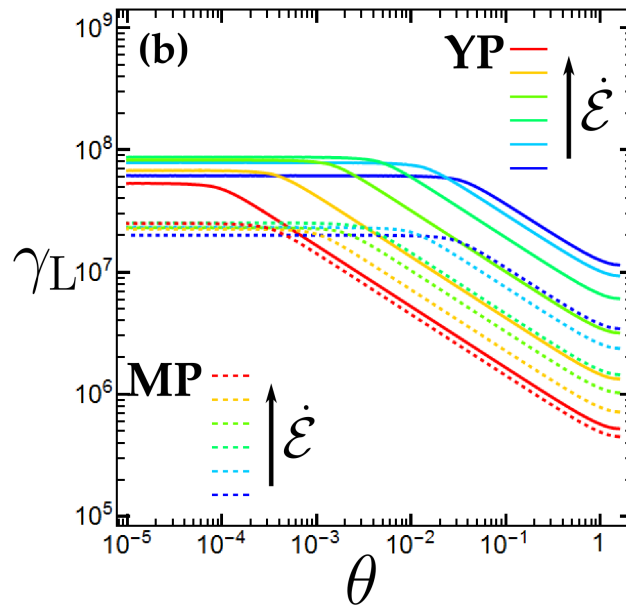
Cerutti et al. 2016

Reverse Engineering

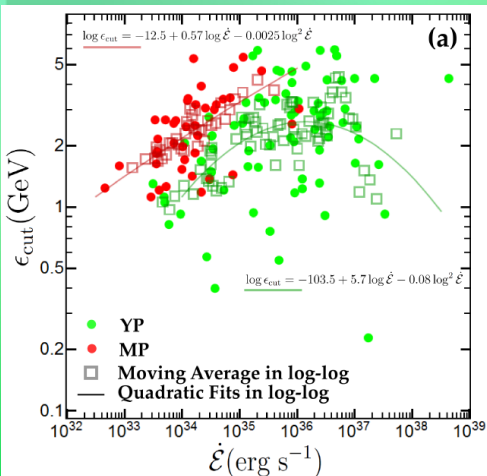
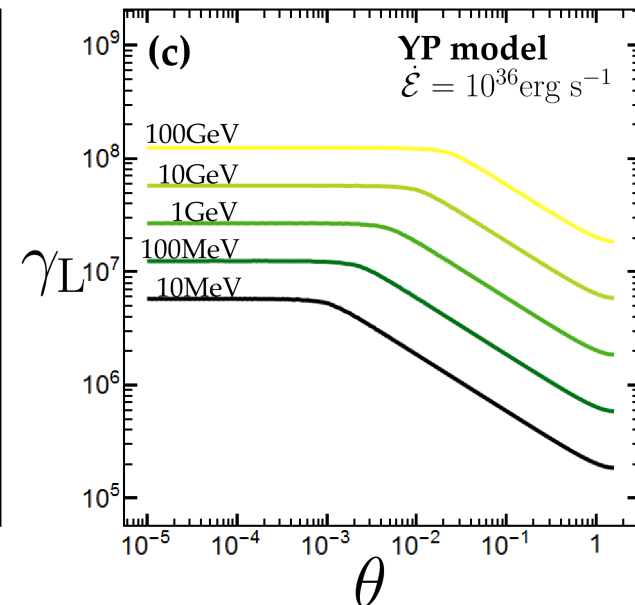
$R_0 = R_{LC}$



$R_0 = 10R_{LC}$



$R_0 = R_{LC}$



$$\epsilon_{cut} = \frac{3}{2} c \hbar \frac{\gamma_L^3}{R_C(\theta)}$$

Kalapotharakos et al. (2019)

$$E, B \sim B_{LC}$$

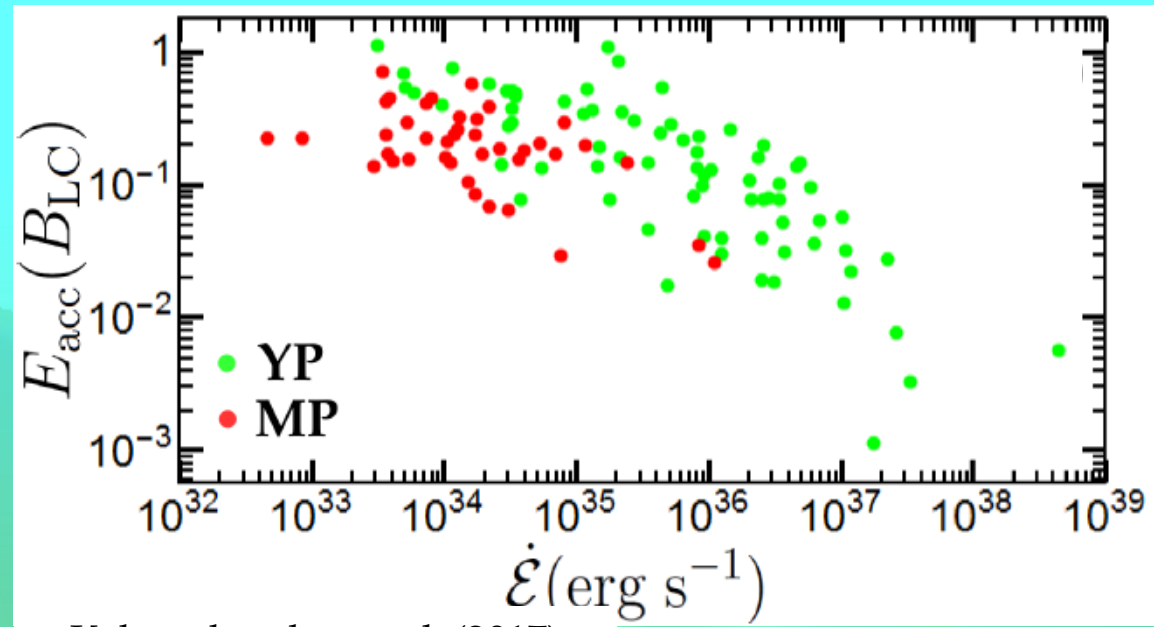
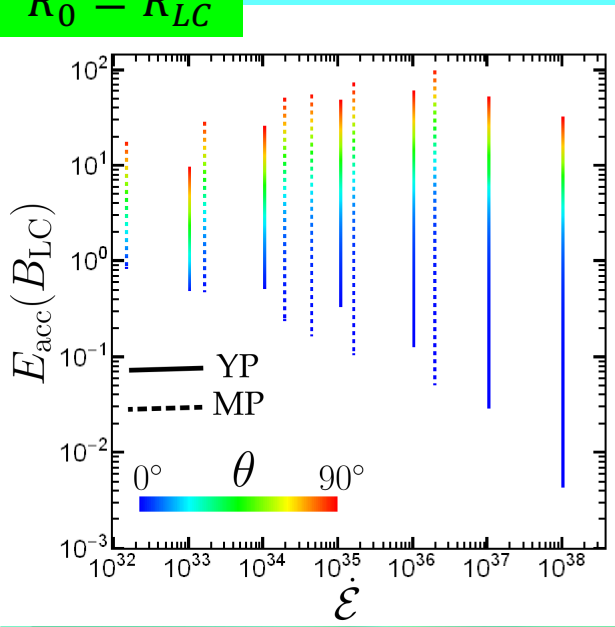
θ decreases:

1. Radiation reaction losses
2. Acceleration

θ should be sustained by another process (e.g. heating)

Reverse Engineering

$$R_0 = R_{LC}$$



Kalapothisarakos et al. (2017)

$$\frac{2q_e^2 \gamma_L^4}{3m_e c R_C(\theta)} = \frac{q_e \mathbf{v} \cdot \mathbf{E}}{m_e c^2}$$

$$\epsilon_{cut} = \frac{3}{2} c \hbar \frac{\gamma_L^3}{R_C(\theta)}$$

Kalapothisarakos et al. (2019)

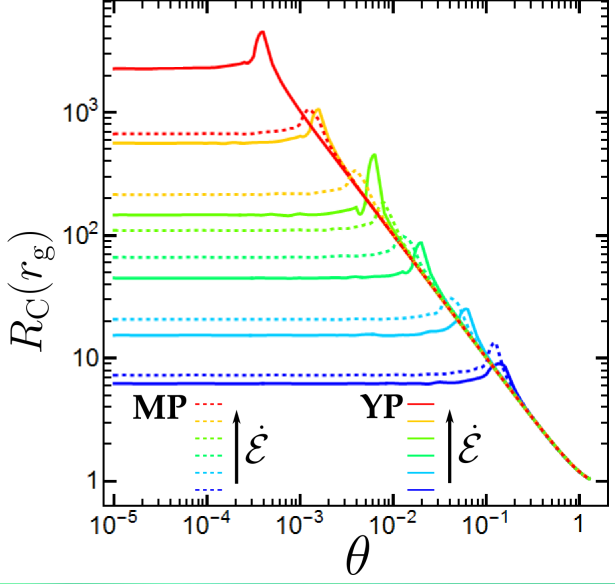
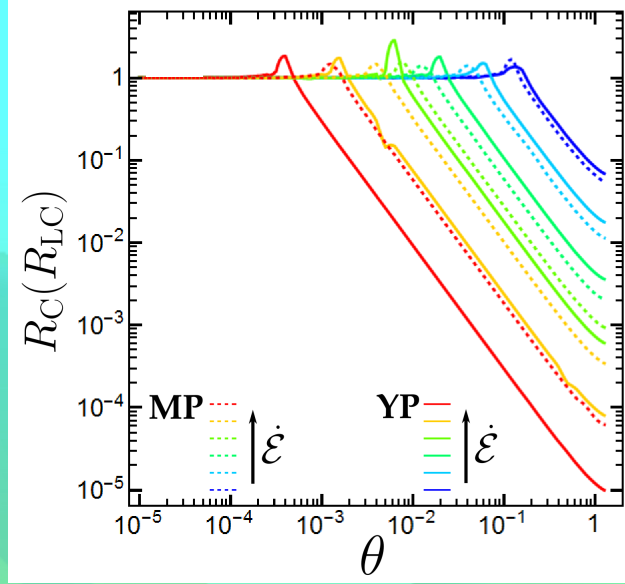
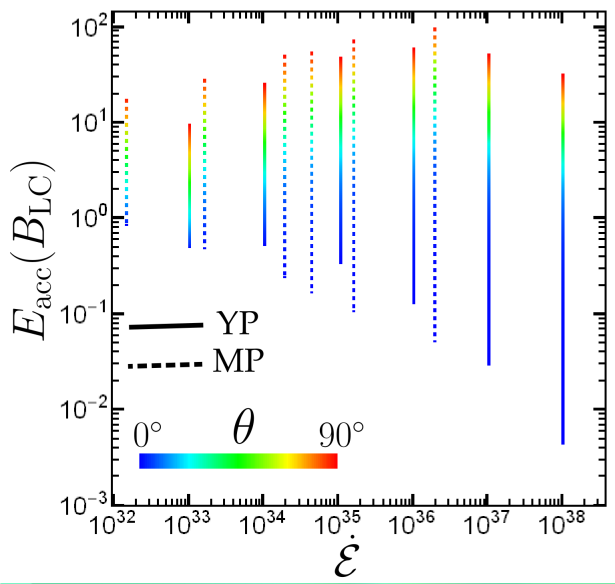
$$E_{acc} < B_{LC}$$

- θ decreases:
1. Radiation reaction losses
 2. Acceleration

θ should be sustained by another process (e.g. heating)

Reverse Engineering

$$R_0 = R_{LC}$$



$$\frac{2q_e^2 \gamma_L^4}{3m_e c R_C(\theta)} = \frac{q_e \mathbf{v} \cdot \mathbf{E}}{m_e c^2}$$

$$\epsilon_{cut} = \frac{3}{2} c \hbar \frac{\gamma_L^3}{R_C(\theta)}$$

Kalapothisarakos et al. (2019)

$$E_{acc} < B_{LC}$$

- θ decreases:
1. Radiation reaction losses
 2. Acceleration

θ should be sustained by another process (e.g. heating)

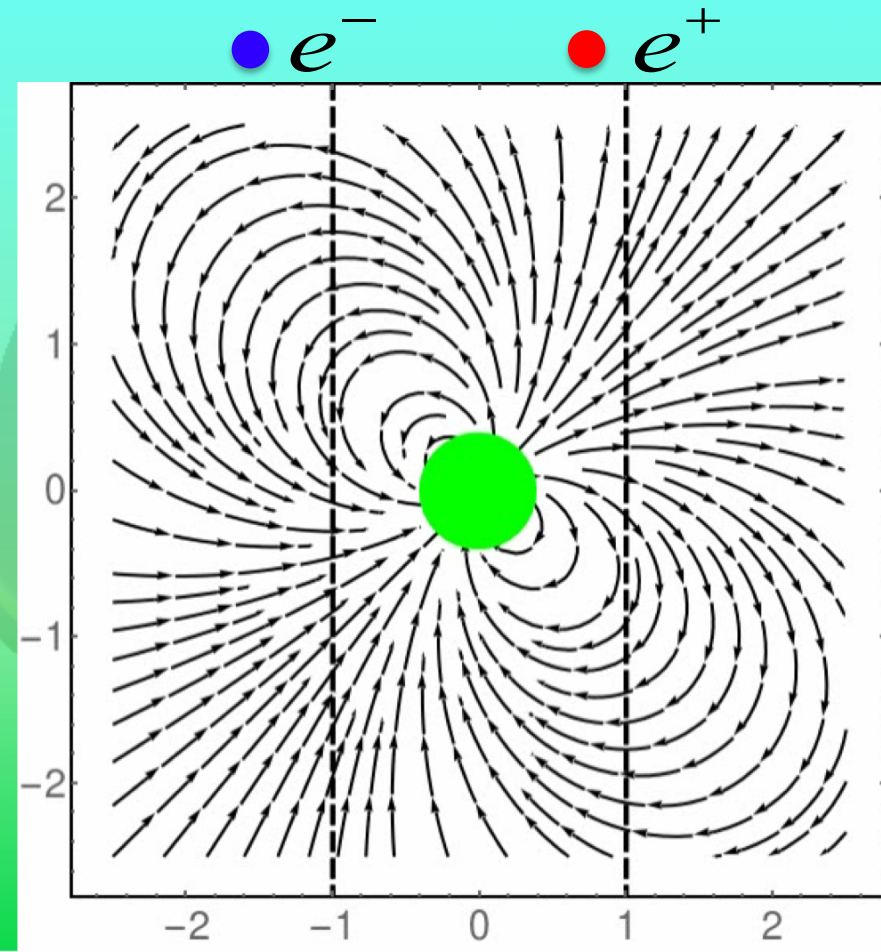
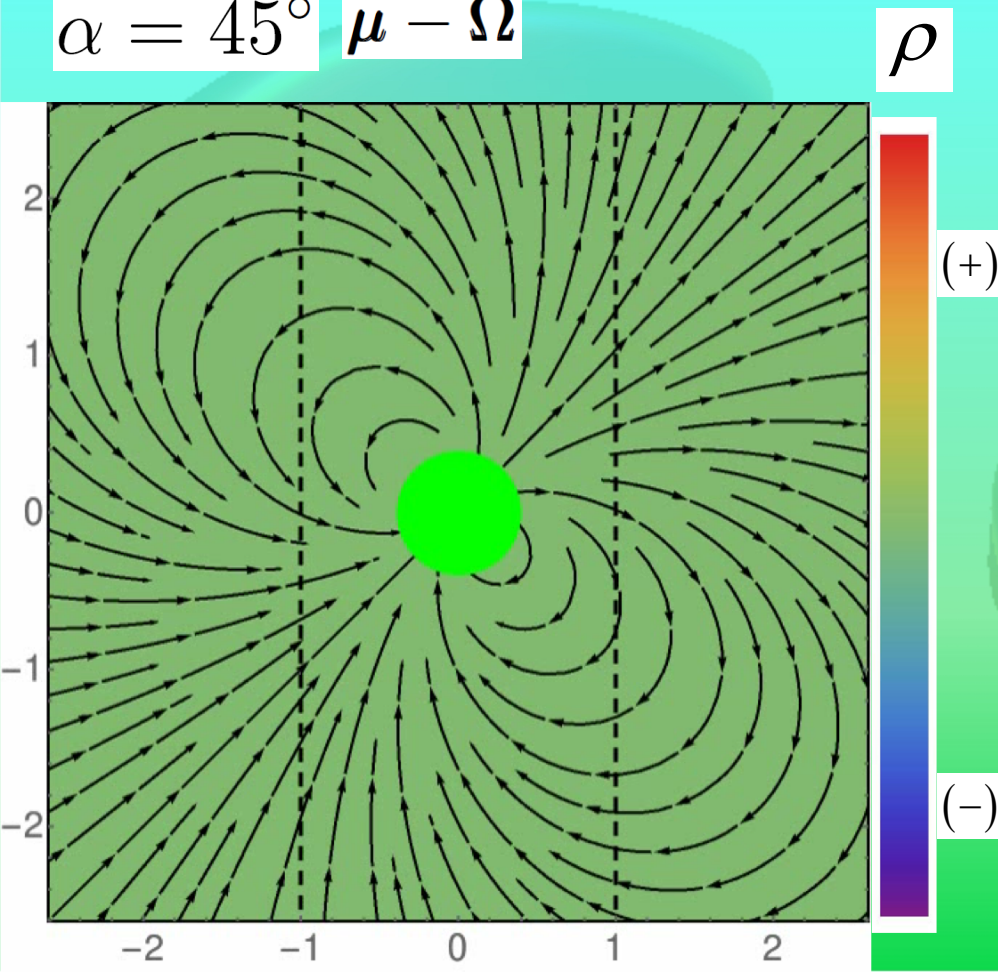
3D Kinetic Models (PIC)

Towards self-consistency:

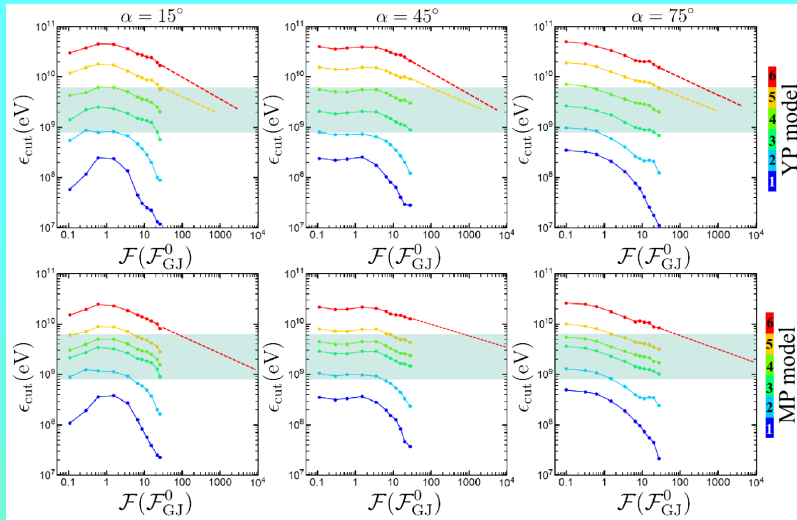
1) Arbitrary particle injection

→ consistent field structure & particle distribution

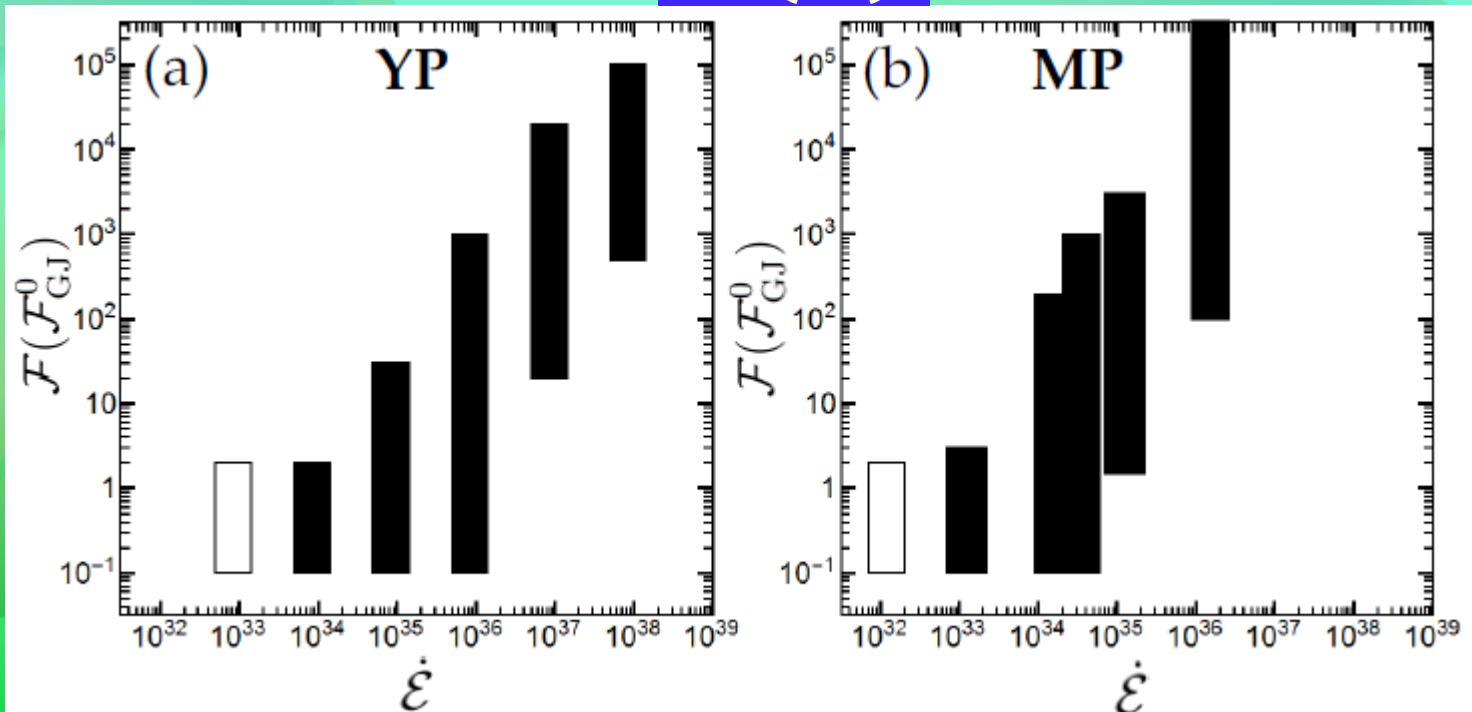
$$\alpha = 45^\circ \quad \mu - \Omega$$



3D Kinetic Models (PIC)



$$\mathcal{F}(\dot{\epsilon})$$



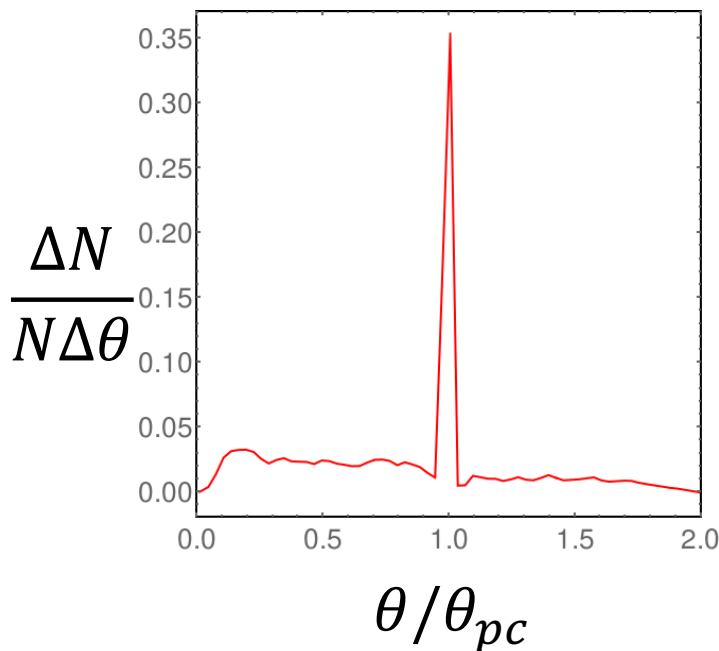
3D Kinetic Models (PIC)

Separatrix injection model

The γ -ray pulsar radiation is mainly regulated by

1. The particle injection rate \mathcal{F}_s along the separatrix
2. The width w of the separatrix zone

Kalapocharakos et al. (in prep)



Requirements

The particle injection rate along the open and the closed field-lines is not very small.

$$(> 5\mathcal{F}_{GJ}^0)$$

However, it is not necessary to be high.

$$(< 10\mathcal{F}_{GJ}^0)$$